

MAPPING EASTERN REDCEDAR (*JUNIPERUS VIRGINIANA* L.) AND QUANTIFYING
ITS BIOMASS IN RILEY COUNTY, KANSAS

by

DAVID RICHARD BURCHFIELD

B.S., Brigham Young University, 2011

A THESIS

submitted in partial fulfillment of the requirements for the degree

MASTER OF ARTS

Department of Geography
College of Arts and Sciences

KANSAS STATE UNIVERSITY
Manhattan, Kansas

2014

Approved by:

Major Professor
Kevin P. Price

Copyright

DAVID RICHARD BURCHFIELD

2014

Abstract

Due primarily to changes in land management practices, eastern redcedar (*Juniperus virginiana* L.), a native Kansas conifer, is rapidly invading onto valuable rangelands. The suppression of fire and increase of intensive grazing, combined with the rapid growth rate, high reproductive output, and dispersal ability of the species have allowed it to dramatically expand beyond its original range. There is a growing interest in harvesting this species for use as a biofuel. For economic planning purposes, density and biomass quantities for the trees are needed. Three methods are explored for mapping eastern redcedar and quantifying its biomass in Riley County, Kansas. First, a land cover classification of redcedar cover is performed using a method that utilizes a support vector machine classifier applied to a multi-temporal stack of Landsat TM satellite images. Second, a Small Unmanned Aircraft System (sUAS) is used to measure individual redcedar trees in an area where they are encroaching into a pasture. Finally, a hybrid approach is used to estimate redcedar biomass using high resolution multispectral and light detection and ranging (LiDAR) imagery. These methods showed promise in the forestry, range management, and bioenergy industries for better understanding of an invasive species that shows great potential for use as a biofuel resource.

Table of Contents

List of Figures	vi
List of Tables	vii
Acknowledgements.....	viii
Dedication.....	ix
Preface.....	x
Chapter 1 - Introduction.....	1
Species Description.....	1
Species Ecology and Human Factors.....	5
Redcedar Uses.....	7
Redcedar Mapping	8
Chapter 2 - Multi-temporal Classification of Eastern Redcedar (<i>Juniperus virginiana</i>) in Eastern Kansas Using a Support Vector Machine (SVM) Classifier	9
Introduction.....	9
Classification of Eastern Redcedar Land Cover with Remote Sensing	10
Support Vector Machine (SVM) Classifier	11
Multi-temporal Classification	13
Methods	13
Study Area	13
Classification.....	14
Results.....	17
Discussion.....	20
Conclusion	21
Chapter 3 - Evaluation of Eastern Redcedar (<i>Juniperus virginiana</i>) Biomass in Eastern Kansas with a Small Unmanned Aircraft System (sUAS).....	23
Introduction.....	23
Remote Sensing with sUAS.....	25
Methods	26
Study Area and Ground Reference Data Collection	26

Flight Preparation.....	27
Zephyr II sUAS.....	28
Sensors	29
Image Processing	31
Discussion.....	33
Chapter 4 - Assessment of Eastern Redcedar (<i>Juniperus virginiana</i>) Biomass Using LiDAR and Multispectral Imagery.....	35
Introduction.....	35
Use of LiDAR and multispectral imagery in forest inventories	37
Methods	39
Study Area	39
LiDAR pre-processing	44
Classification of multispectral imagery	44
Redcedar canopy model development	46
Biomass predictive model and map development	46
Results.....	47
Redcedar Canopy Model.....	47
Biomass Predictive Model	49
Conclusion	50
References.....	51

List of Figures

Figure 1.1 Eastern redcedar encroaching in a pasture near Russell, KS.....	1
Figure 1.2 Eastern redcedar foliage.	2
Figure 1.3 Range of eastern redcedar in the United States (derived from Little, 1971).	3
Figure 1.4 An example of redcedar (dark areas on the images) expansion in Riley County, KS, 1962 (top) to 2012 (bottom). (Images courtesy of USDA NAIP Program and KSU Historical Aerial Photo Archive)	4
Figure 1.5 Eastern redcedar trees catching fire during a prairie burn. Image courtesy of the Kansas Forest Service.	6
Figure 1.6 Area of concern in Manhattan, KS, where a neighborhood borders a large redcedar stand (outlined in yellow). Redcedar stands encroaching in developed areas pose a high risk due to greater wildfire potential. Image courtesy of the USDA NAIP program.	7
Figure 1.7 Eastern redcedar logs and mulch processed for gardening use near Pratt, Kansas. Image courtesy of Larry Biles.....	8
Figure 2.1 Histogram from Landsat TM Band 4 (NIR band) for Riley County, Kansas from August 1, 2011.	11
Figure 2.2 Illustration of Support Vector Machine (SVM) operation in a spectral feature space. From Mountrakis, et al., 2011.....	12
Figure 2.3 False-color composite (4-3-2) Landsat TM images of Riley County, Kansas from January 5, 2011 (top) and August 1, 2011 (bottom).	16
Figure 2.4 Illustration of multi-temporal image stacking method.	17
Figure 2.5 Multi-temporal Support Vector Machine (SVM) classification of Riley County, KS. 19	
Figure 2.6 High-resolution (1-meter spatial resolution) false-color composite of a neighborhood in Manhattan, Kansas, showing spectral difference between Eastern redcedar cover and broadleaf deciduous tree cover in June 2012. Redcedar cover is outlined by a 30m (spatial resolution) multi-temporal Landsat classification (yellow). Note dark spectral characteristics of redcedar versus bright appearance of neighboring broadleaf tree cover. Image courtesy USDA NAIP program.	21
Figure 3.1 Graph showing the allometric relationship between redcedar canopy area (m ²) and wet total aboveground biomass (kg). The resulting regression equation is also shown.....	27

Figure 3.2 UAS pilot (Dr. Deon van der Merwe) preparing the Ritewing Zephyr II sUAS for flight. Photograph courtesy of Joel Prince.	29
Figure 3.3 Sample color-infrared image taken by the Canon PowerShot S100 camera over the study area showing redcedar trees (A), deciduous forest (B), and tallgrass prairie areas (C).	30
Figure 3.4 Video frame from the GoPro HD Hero2 video camera taken over the study area.....	31
Figure 3.5 Orthophoto mosaic of the study area produced by Agisoft Photoscan Professional software. This mosaic incorporates data from approximately 180 individual images that represented approximately 93 ha of ground area. Note the presence of seamlines in portion of the mosaic caused by variable cloud conditions.....	32
Figure 3.6 Polygons are drawn around the canopy of each redcedar to measure their canopy area using ArcGIS software.....	33
Figure 3.7. sUAS remote sensing workflow used in this project.....	34
Figure 4.1 Eastern redcedar in Riley County, Kansas.	36
Figure 4.2 Illustration of multiple returns from a LiDAR pulse within a tree canopy. From Stoker (date unknown).	38
Figure 4.3 Redcedar classification and biomass mapping workflow.	40
Figure 4.4 Map of Riley County, Kansas showing study plot locations.....	42
Figure 4.5 Allometric equation relating diameter at breast height (DBH) to biomass.	43
Figure 4.6 Aerial schematic of the modified point-center quarter sampling method at a study site.	43
Figure 4.7 Redcedar canopy height model (LiDAR) vs. mean redcedar height in ground reference plots.	48
Figure 4.8 Aerial percent cover vs. ground canopy cover (measured with densiometer).	49

List of Tables

Table 2.1 Confusion matrices for each classification: winter (top), summer (middle), and multi-date (bottom).	18
Table 4.1 Summary of site measurements for each ground reference plot.....	41
Table 4.2 Accuracy assessment summary of the redcedar biomass prediction model.	50

Acknowledgements

I would like to acknowledge the support of the Kansas Forest Service in funding this research and lending their equipment, assistance, and forestry expertise to the field work and other portions of the project. This research would not have been possible without their support. I would also like to recognize and thank Kevin Price and Robert Daniels for applying for the grant from the Kansas Forest Service that supported this research.

Johnny Bryant collaborated with me on much of this work, particularly the fourth chapter of my thesis, on which we are co-authors. Johnny's extensive knowledge of biology and statistics greatly enhanced the quality of this research. He also kept me laughing when field work got hot and tedious. I would like to thank him and recognize him for his crucial role in this project.

The UAS flight required extensive planning, and I would like to thank Deon van der Merwe (UAS pilot) and Kirk Demuth (Pilot-in-Command) for their help with planning the mission, submitting the FAA Certificate of Authorization for the flight, and piloting the Zephyr II UAS, which was custom-designed and built by Deon. I would also like to express appreciation to Clenton Owensby for allowing us to access the Rannells Tallgrass Prairie Preserve for the UAS flight.

I would also like to acknowledge the kind assistance of those who volunteered their time to aid Johnny and me in the field work portion of the project during the sweltering summer of 2012—Kevin Price, Sri Sankar, Chris Burchfield, Jason Hartman, and Nate Wold. Thanks also go to those who allowed us to access their property for the field work, including Mr. Charles Hall (Ranch of the Prairie Rose), The Master Teacher, and the Kansas Farm Bureau.

I would also like to thank Kevin Price, Johnny Bryant, Lynn Brien, Nan An, LeAnn Burchfield, and Richard Miller for their assistance with proofreading. I am also appreciative of the support of my graduate committee members—Kevin Price, Deon van der Merwe, and Doug Goodin.

Dedication

This thesis is dedicated to family members, friends, and colleagues who made this work possible. I would like to also dedicate this work to my wife Rachael, who has been a wonderful support to me during this entire process.

Preface

“There is not any kind of wood in all these plains, away from the gullies and rivers, which are very few.”

–Francisco Coronado’s journal entry describing a prairie in Kansas as he traversed the region in 1541 (quoted in Bragg & Hulbert, 1976).

Chapter 1 - Introduction

In recent decades, woody tree invasion has become a serious problem in the tallgrass prairie region of Eastern Kansas (Bragg & Hulbert, 1976). Because of rapid human settlement, overgrazing, and fire suppression, woody species have invaded sites that were once healthy tallgrass prairies (Briggs, *et al.*, 2002). Among the most invasive of these woody species is *Juniperus virginiana*, commonly known as eastern redcedar (Figure 1.1).



Figure 1.1 Eastern redcedar encroaching in a pasture near Russell, KS.

Species Description

Eastern redcedar (known hereafter as “redcedar”) is the only juniper species native to the state of Kansas (Pease, 2007). It is a species characterized by its rapid growth and high reproductive output (Briggs, *et al.*, 2002). Redcedar is a coniferous species that has sharp, scaly leaves that perform photosynthesis (Stevens, *et al.*, 2005) (Figure 1.2). Unlike deciduous trees

that lose their leaves during autumn, redcedar retains its leafy material throughout the year. Redcedar is a dioecious species—female redcedars can be identified by the presence of small, round, waxy blue seed cones (often called “berries”) during certain times of the year (Van Haverbeke & Read, 1976; Stevens, *et al.*, 2005).



Figure 1.2 Eastern redcedar foliage.

The range of redcedar is extensive, spanning the eastern half of the United States from the Atlantic to the High Plains and from Texas in the south to Ontario in the north (Figure 1.3). Isolated patches of redcedar have also been reported in Oregon. In Kansas, eastern redcedar grows primarily in the eastern two-thirds of the state where conditions are humid enough to support it (Stevens, *et al.*, 2005). It is also widely planted as a “backbone” windbreak species in Kansas (Strine, 2004). Due in part to these windbreak plantings across the state, the current range of redcedar exceeds its historical range (Owensby, *et al.*, 1973).

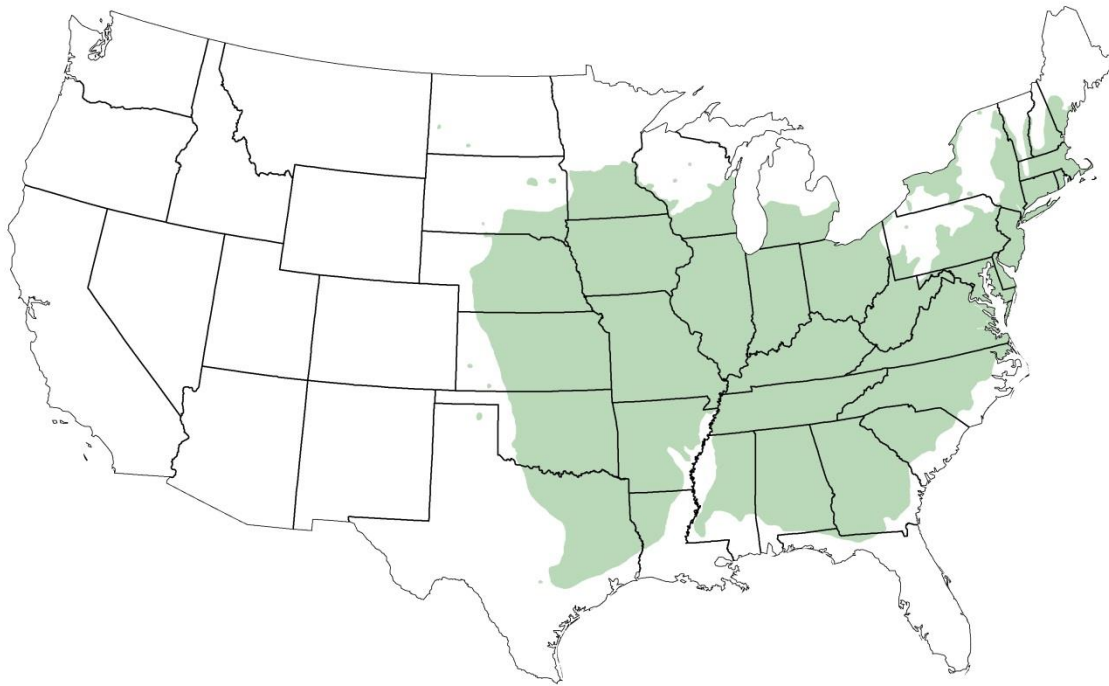


Figure 1.3 Range of eastern redcedar in the United States (derived from Little, 1971).

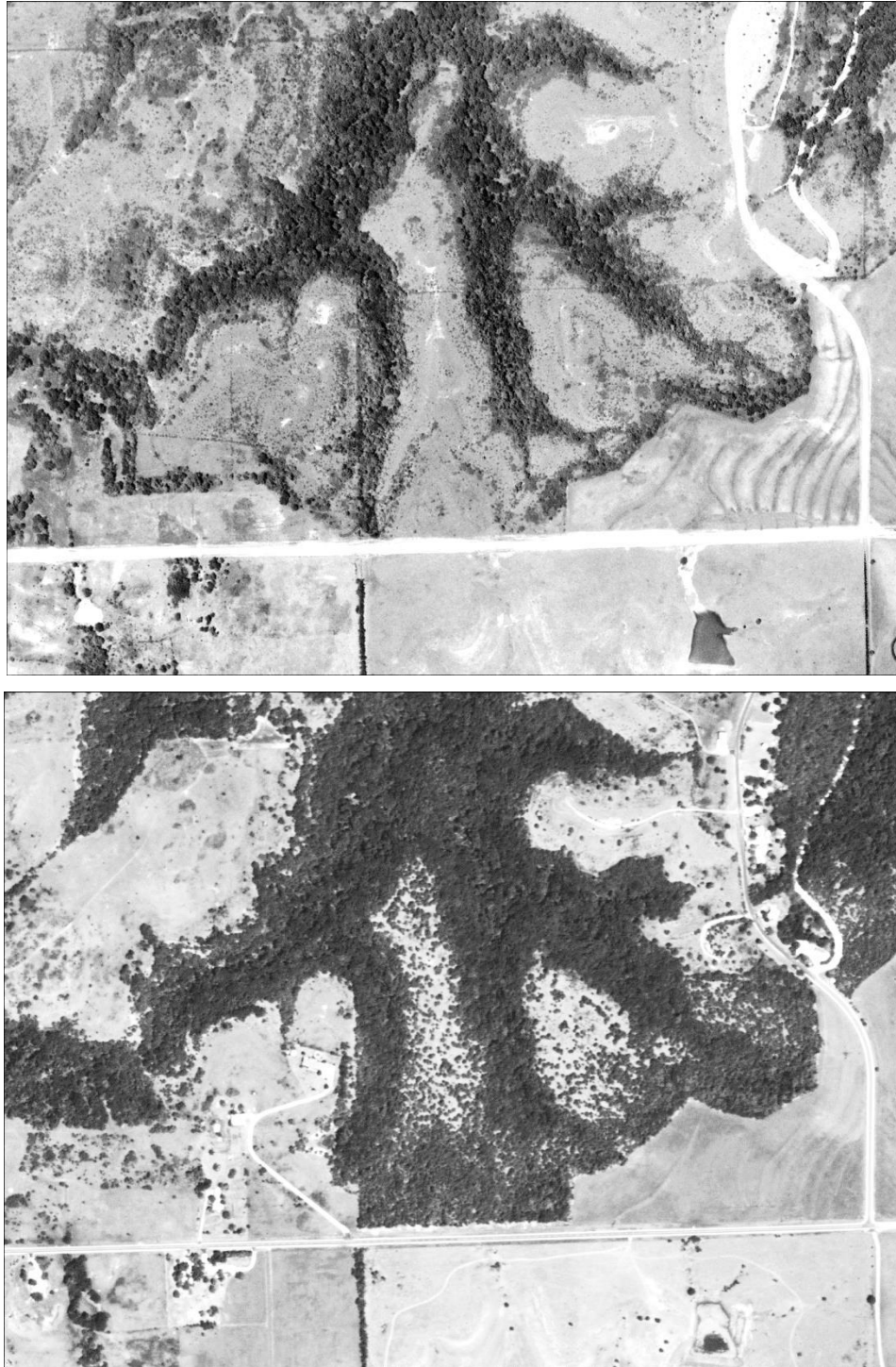


Figure 1.4 An example of redcedar (dark areas on the images) expansion in Riley County, KS, 1962 (top) to 2012 (bottom). (Images courtesy of USDA NAIP Program and KSU Historical Aerial Photo Archive)

Species Ecology and Human Factors

Eastern redcedar is a pioneer invader species that will readily spread over a short period of time (Van Haverbeke & Read, 1976). Prior to European settlement in Kansas, woody species (including redcedar) were primarily located in stream bottoms (lowlands) in the Flint Hills region (Bragg & Hulbert, 1976). The Spanish explorer Coronado wrote in 1541 as he travelled through the region, “There is not any kind of wood in all these plains, away from the gullies and rivers, which are very few” (Bragg & Hulbert, 1976). Before settlement occurred in the region, as woody species would spread into upland areas, they were naturally controlled by periodic wildfires. Using dendrochronological dating methods, these fires have been shown to have burned on average every four years in the Flint Hills prior to European-American settlement (Allen & Palmer, 2011). Since Europeans settled the historic range of redcedar, they have fragmented the landscape, constructing artificial barriers to fire (primarily roads) that have halted the natural progression of prairie fires (Briggs, *et al.*, 2002). Poor land management and plantings of redcedar in windbreaks have further accelerated its spread (Owensby, *et al.*, 1973). These factors have caused redcedar to become established in upland tallgrass prairies.

Redcedar’s invasiveness has become a problem in the Flint Hills region where many absentee landowners have acquired land as an investment or for hunting (Kindscher & Scott, 1997). These landowners may often be unwilling or unable to take the necessary steps—such as conducting annual prairie burns—to properly manage their property. As redcedar has spread into the uplands due to a lack of fire to control it, it has often turned into dense stands that crowd out warm-season (C₄) native tallgrass prairie grasses and forbs (Gehring & Bragg, 1992) (Figure 1.4). Many of these species are important forage plants for grazing animals in Kansas. Valuable rangelands can be converted into closed-canopy redcedar stands in as little as 40 years (Briggs, *et al.*, 2002). Beef cattle ranching is an important industry in Kansas, representing \$8.5 billion out of the \$14.4 billion agricultural industry in the state (USDA, 2011), and this industry is being threatened by the spread of redcedar into rangelands.

Another major concern with redcedar is its encroachment into populated areas. Redcedar foliage contains flammable volatile oils, and dense stands of redcedar located in urban and suburban areas can increase the risk of a wildfire affecting populated areas (Ward, 2013) (Figure 1.5) (Figure 1.6).



Figure 1.5 Eastern redcedar trees catching fire during a prairie burn. Image courtesy of the Kansas Forest Service.



Figure 1.6 Area of concern in Manhattan, KS, where a neighborhood borders a large redcedar stand (outlined in yellow). Redcedar stands encroaching in developed areas pose a high risk due to greater wildfire potential. Image courtesy of the USDA NAIP program.

Redcedar Uses

Eastern redcedar has been shown to be a useful species in industry and agriculture. It is commonly harvested for construction of pencils and wood chests, and it is also chipped into mulch for use in landscaping and gardening (Van Haverbeke & Read, 1976) (Figure 1.7). Redcedar oil has also been extracted for use in the essential oil industry (Gawde, *et al.*, 2009; CAFNRnews, 2008; Semen & Hiziroglu, 2005). It has also been shown to contain a high amount of energy for heating. Large individual trees have been shown to contain over twelve million British Thermal Units (BTUs) of energy, equivalent to around 106 gallons of heating oil, or 0.6 tons of anthracite coal (Strauss, *et al.*, 2011; Slusher, 1995). It has been proposed that redcedar could be harvested for use as a biofuel, providing an inexpensive, locally-obtained fuel source

for Kansas. Redcedar wood can be converted into biodiesel, wood chips for wood burning boilers, or “biochar,” a charcoal soil amendment (Teel, 2012; Starks, *et al.*, 2011).



Figure 1.7 Eastern redcedar logs and mulch processed for gardening use near Pratt, Kansas. Image courtesy of Larry Biles.

Redcedar Mapping

To facilitate development of an eastern redcedar biofuel industry in Kansas, redcedar cover and biomass estimates are needed on a detailed scale for economic planning purposes. The purpose of this thesis is to explore three methods of measuring redcedar biomass and cover:

1. To classify redcedar cover on the landscape using moderate spatial resolution (30-meter) Landsat TM satellite imagery in order to identify large stands where commercial harvesting could be viable.
2. To quantify the biomass of individual redcedar trees in an automated fashion using high spatial resolution aerial imagery collected using a small unmanned aircraft system.
3. To map redcedar biomass across a large area (*e.g.* a county) using a fusion of satellite imagery, LiDAR data, and high spatial resolution color-infrared aerial photography.

Chapter 2 - Multi-temporal Classification of Eastern Redcedar (*Juniperus virginiana*) in Eastern Kansas Using a Support Vector Machine (SVM) Classifier

Introduction

In recent decades, woody tree invasion has become a serious problem in the tallgrass prairie region of Eastern Kansas (Bragg & Hulbert, 1976). Because of rapid human settlement, overgrazing, and fire suppression, woody species have invaded sites that were once healthy tallgrass prairies (Briggs, *et al.*, 2002). Among the most invasive of these woody species is *Juniperus virginiana*, commonly known as eastern redcedar (Figure 1.1).

Eastern redcedar is a pioneer invader species that will readily spread over a short period of time (Van Haverbeke & Read, 1976). Prior to European settlement in Kansas, woody species (including redcedar) were primarily located in stream bottoms (lowlands) in the Flint Hills region (Bragg & Hulbert, 1976). The Spanish explorer Coronado wrote in 1541 as he travelled through the region, “There is not any kind of wood in all these plains, away from the gullies and rivers, which are very few” (Bragg & Hulbert, 1976). Before settlement occurred in the region, as woody species would spread into upland areas, they were naturally controlled by periodic wildfires. Using dendrochronological dating methods, these fires have been shown to have burned on average every four years in the Flint Hills prior to European-American settlement (Allen & Palmer, 2011). Since Europeans have settled the historic range of redcedar, they have fragmented the landscape, constructing artificial barriers to fire (primarily roads) that have halted the natural progression of prairie fires, allowing redcedar to expand its presence (Briggs, *et al.*, 2002). Poor land management and plantings of redcedar in windbreaks have further accelerated its spread (Owensby, *et al.*, 1973). These factors have caused redcedar to become established in upland tallgrass prairies.

Redcedar’s invasiveness has become a problem in the Flint Hills region in north-central Kansas where many absentee landowners have acquired land as an investment or for hunting (Kindscher & Scott, 1997). These landowners may often be unwilling or unable to take the necessary steps—such as conducting annual prairie burns—to properly manage their property. As redcedar has spread into the uplands due to a lack of fire to control it, it has often turned into

dense stands which crowd out warm-season (C_4) native tallgrass prairie grasses and forbs (Gehring & Bragg, 1992). Many of these species are important forage plants for grazing animals in Kansas. Valuable rangelands can be converted into closed-canopy redcedar stands in as little as 40 years (Briggs, *et al.*, 2002). Beef cattle ranching is an important industry in Kansas, representing \$8.5 billion out of the \$14.4 billion agricultural industry in the state (USDA, 2011), and this industry is being threatened by the spread of redcedar into rangelands.

Another major concern with redcedar is its encroachment into populated areas. Redcedar foliage contains flammable volatile oils, and dense stands of redcedar located in urban and suburban areas can increase the risk of a wildfire affecting built-up areas (Ward, 2013).

Despite its invasiveness, eastern redcedar has been shown to be a useful species in industry and agriculture. It is commonly harvested for construction of pencils and wood chests, and it is also chipped into mulch for use in landscaping and gardening (Van Haverbeke & Read, 1976). Redcedar oil has also been extracted for use in the essential oil industry (Gawde, *et al.*, 2009; CAFNRnews, 2008; Semen & Hizirolu, 2005). It has also been shown to contain a high amount of energy for heating. Large individual trees have been shown to contain over twelve million British Thermal Units (BTUs) of energy, equivalent to around 106 gallons of heating oil, or 0.6 tons of anthracite coal (Strauss, *et al.*, 2011; Slusher, 1995). It has been proposed that redcedar could be harvested for use as a biofuel, providing an inexpensive, locally-obtained fuel source for Kansas. Redcedar wood can be converted into biodiesel, wood chips for wood burning boilers, or “biochar,” a charcoal soil amendment (Teel, 2012; Starks, *et al.*, 2011). To facilitate development of a redcedar biofuel industry in Kansas, accurate acreage estimates and location data are needed so that harvesting resources may be efficiently allocated.

Classification of Eastern Redcedar Land Cover with Remote Sensing

In the past, systematic random ground surveys have been conducted in Kansas to evaluate forest resources (Moser, *et al.*, 2008). These surveys have taken place on an intermittent basis in Kansas since 1936 (Raile & Spencer, 1984). Ground sampling schemes are slow and costly, and can be inaccurate at characterizing forest species composition at a regional or county level, due to the spatially random nature of the sampling scheme (Bechtold & Patterson, 2005). Remote sensing methods can be used to improve upon ground sampling methods (Jensen, 1983).

Satellite remote sensing is used extensively as a land use/land cover measurement tool (Anderson, *et al.*, 1976), and has been shown to be invaluable for identifying and monitoring changes in vegetated land cover, such as rangelands and forests (Jensen, 2007; Booth & Tueller, 2003; Briggs, *et al.*, 2002). Remote sensing techniques have been widely used for monitoring the expansion of invasive plant species, including *Juniperus* species like eastern redcedar (Sankey & Germino, 2008; Sankey, *et al.*, 2010; Everitt, *et al.*, 2001; Starks, *et al.*, 2011; Thayn & Price, 2006).

Support Vector Machine (SVM) Classifier

The problem of classifying land covered by eastern redcedar necessitates the use of an appropriate classification algorithm. Redcedar stands tend to cover small areas (generally less than 10 ha in size) where the land has been poorly managed. Redcedar may be present on one parcel and absent on adjacent parcels, and large, homogeneous training areas are difficult to find, making the most common classification algorithms (ISODATA, Maximum Likelihood) less than ideal because they work best when large training datasets are available (Richards & Jia, 2006). The most common classifiers also tend to be designed for normal (parametric) datasets (Richards & Jia, 2006), and satellite imagery often contains non-parametric data with multiple peaks in the histogram that represent different land cover types (Figure 2.1). It has been shown that classifications of non-normal datasets perform better when non-parametric classifiers (such as SVM) are used.

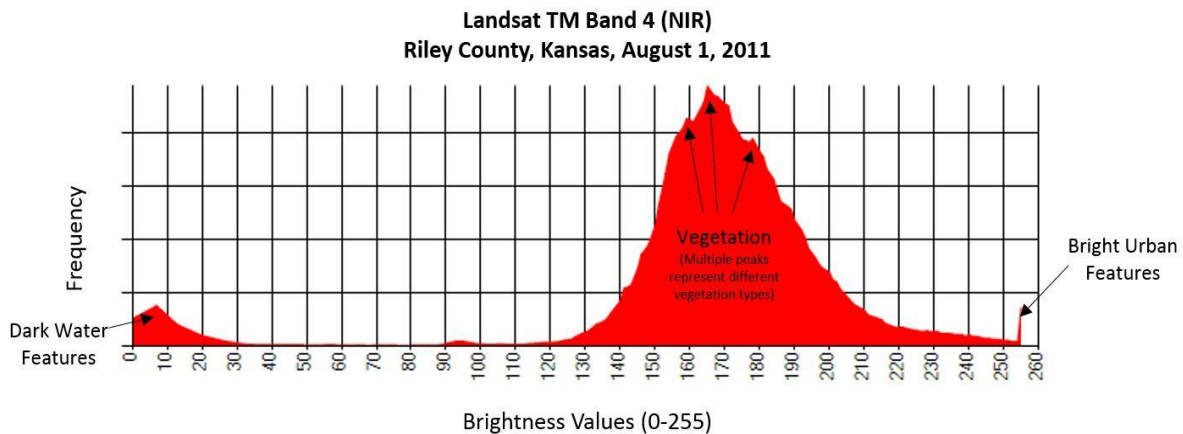


Figure 2.1 Histogram from Landsat TM Band 4 (NIR band) for Riley County, Kansas from August 1, 2011.

The use of SVM classifiers for land cover classification has increased in popularity within the remote sensing community over the past several years (Melgani, *et al.*, 2004; Pal, *et al.*, 2005; Mountrakis, *et al.*, 2011). An SVM is a non-parametric classifier that handles small training samples well and often returns higher accuracies than traditional image classification methods. The SVM algorithm separates data into classes by placing a hyperplane between “support vectors” to represent the boundaries between two classes in a spectral feature space (Mountrakis, *et al.*, 2011; Richards & Jia, 2006) (Figure 2.2). Because of the characteristics of redcedar cover within the study area, SVM was considered to be an appropriate classification algorithm for this study.

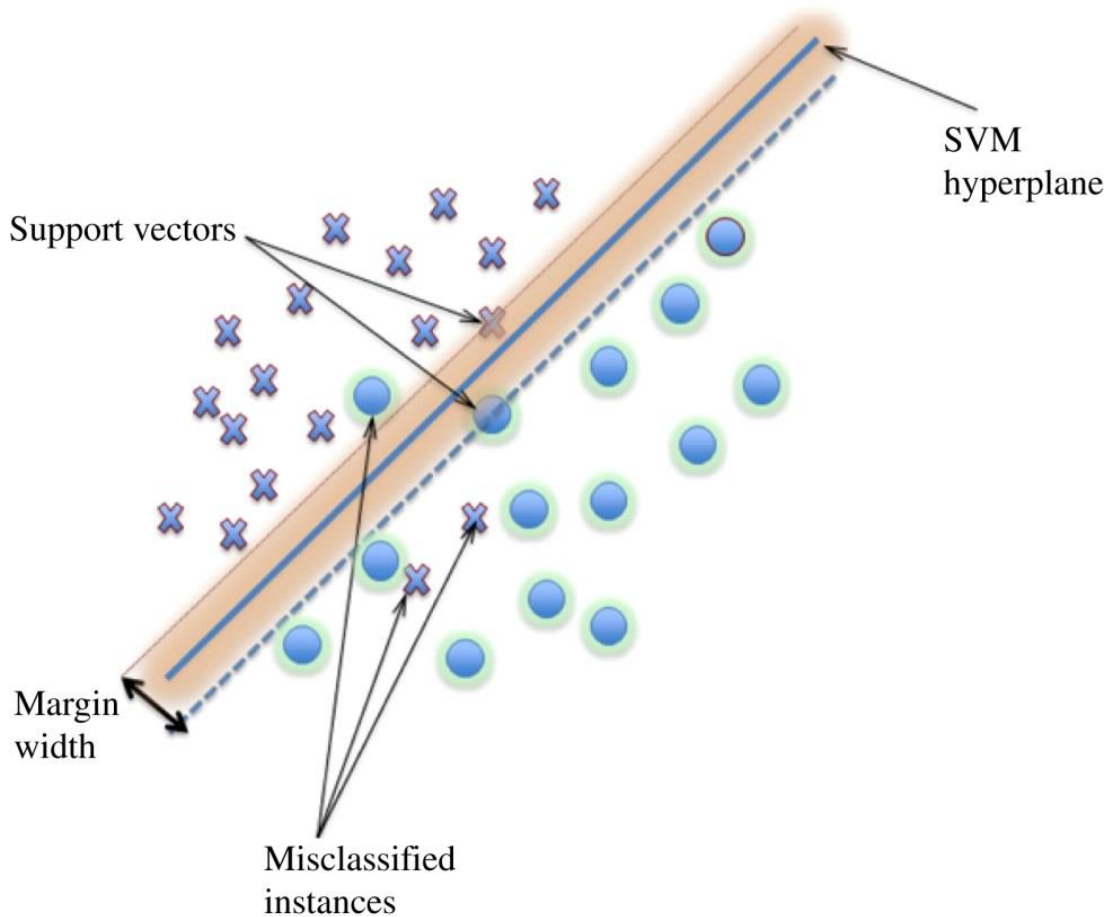


Figure 2.2 Illustration of Support Vector Machine (SVM) operation in a spectral feature space. From Mountrakis, et al., 2011.

Multi-temporal Classification

The seasonal characteristics of eastern redcedar introduce another challenge to accurate land cover classification. Eastern redcedar is an evergreen species, so its spectral characteristics remain relatively constant throughout the year when compared to surrounding cover types, such as deciduous forest. A single-date classification may confuse redcedar with other photosynthetically-active cover types (deciduous forest, grasslands, and crops in the summer, and winter wheat in the winter).

Multi-temporal (or multi-seasonal) classifications have been shown to be effective for improving classification accuracy of vegetated land cover types (Price, *et al.*, 1997). These methods introduce a “stack” of images from different dates (*e.g.* summer and winter dates) in order to account for seasonal variability in the spectral characteristics of vegetation within a given year. Multi-temporal classification has been used in other studies to overcome the problem of single-date class confusion, improving classification accuracies for various land cover types, including agricultural lands and rangelands (Price, *et al.*, 1997; Langley, *et al.*, 2001; Guo, *et al.*, 2003). Similar multi-temporal classification techniques have previously been applied to forest classifications with varying degrees of success (Raines, *et al.*, 2008; McCleary, *et al.*, 2008; Wolter, *et al.*, 1995).

The goals of this study were to:

- 1) Develop automated classification methods for mapping eastern redcedar land cover using a support vector machine classifier, and
- 2) Determine if a multi-temporal approach improved classification accuracy.

Methods

Study Area

The project study area, Riley County, Kansas, was identified by the Kansas Forest Service as a county of concern due to its high rate of redcedar encroachment. An unpublished study estimated a 23,000% increase of redcedar cover in Riley County between 1965 and 2005 (Grabow & Price, 2010). Riley County lies within the Flint Hills ecoregion. Portions of the county are topographically rugged, with steep stream banks punctuating rocky upland areas. The native vegetation consists of tallgrass prairie species—primarily big bluestem (*Andropogon gerardii*), indianguass (*Sorghastrum nutans*), and little bluestem (*Andropogon scoparius*)—in the

uplands. Trees, including hackberry (*Celtis occidentalis*), American elm (*Ulmus americana*), green ash (*Fraxinus pennsylvanica*), and black walnut (*Juglans nigra*) are found along the stream bottoms (Owensby, 2014). The elevation ranges from 298 meters in the Kansas River Valley to 464 meters in the west-central portion of the county. Tuttle Creek Reservoir (along the Big Blue River) is a dominant feature in the county. Manhattan, the county seat and home of Kansas State University, is the largest city. The total area of the county is 1611 km² (U.S. Census Bureau, 2013), the majority of which is utilized for cattle grazing and crop production. The climate in Riley County is classified as humid continental (Köppen *Dfa*) (Peel, *et al.*, 2007).

Classification

Cloud-free 30-meter resolution Landsat TM imagery was acquired for Riley County, Kansas for January 5, 2011 (winter) and August 1, 2011 (summer) (Figure 2.3). For each image date, Landsat TM bands 1–5 and 7 were layer stacked, clipped to a county boundary Shapefile, and radiometrically calibrated using the Dark Object Subtraction tool in ENVI 5®. To combine data from both dates, the resulting stacked and calibrated images were integrated into a single 12 band TIFF image using ENVI 5 (Figure 2.4). The thermal band was excluded from the dataset.

Training samples were then selected from U.S. Department of Agriculture (USDA) National Agricultural Imagery Program (NAIP) imagery (1.0 meter spatial resolution) because homogeneous training areas could be more easily delineated using NAIP imagery versus Landsat TM imagery. A modified version of the Anderson classification scheme (Anderson, *et al.*, 1976) was used to categorize the training samples, which represented Agricultural Land, Deciduous Forest, Evergreen Forest (primarily consisting of eastern redcedar in the study county), Rangeland, Urban, Water, and Wetland.

The training data were used as the input in the Support Vector Machine Classifier tool in ENVI 5, and the process was repeated for each image—summer, winter, and multi-seasonal—for comparison purposes. Input parameters were unchanged from the default values—a radial basis function was used as the kernel type, the gamma value was 0.083 (inverse of the number of computed attributes), the penalty parameter was 100.0, and the probability threshold was zero, meaning that all pixels would be classified. Classification times ranged from two to five minutes using these settings on a typical workstation computer. Following classification, 25 random

samples representing each of the seven classes were selected from the classified images and compared with NAIP imagery in order to evaluate the accuracy of each classification.



Figure 2.3 False-color composite (4-3-2) Landsat TM images of Riley County, Kansas from January 5, 2011 (top) and August 1, 2011 (bottom).

Results

Of the three classifications (summer, winter, and multi-seasonal), the multi-seasonal classification performed best for classifying eastern redcedar cover, yielding a producer's accuracy of 93% and a user's accuracy of 100%. The overall accuracy of the classification (including non-forested land cover classes) was 81% (Table 2.1) (Figure 2.5). Between the summer and winter classifications, the summer classification performed best for classifying redcedar cover, yielding a producer's accuracy of 94% and a user's accuracy of 68%, with an overall accuracy of 73%. The winter classification produced redcedar cover producer's, user's, and overall accuracy values of 79%, 76%, and 69%, respectively. Kappa statistics for the classifications were 68% (summer), 64% (winter), and 77% (multi-seasonal).

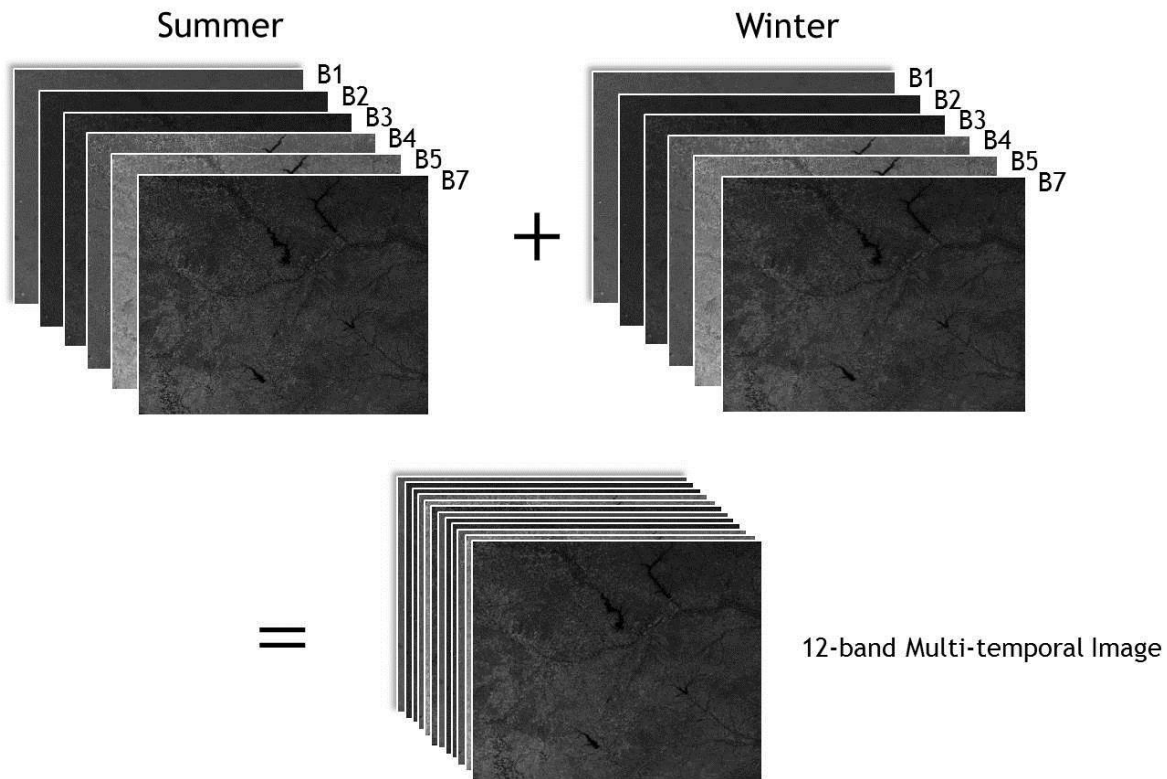


Figure 2.4 Illustration of multi-temporal image stacking method.

Table 2.1 Confusion matrices for each classification: winter (top), summer (middle), and multi-date (bottom).

Winter		Reference Data							
(January 5, 2011)		Urban	Deciduous	Redcedar	Ag Land	Rangeland	Wetland	Water	Total
Classification Data	Urban	23	0	0	1	1	0	0	25
	Deciduous	0	17	5	0	3	0	0	25
	Redcedar	0	5	19	0	1	0	0	25
	Ag Land	1	0	0	19	5	0	0	25
	Rangeland	0	1	0	5	17	2	0	25
	Wetland	0	12	0	1	9	2	1	25
	Water	0	1	0	0	0	0	24	25
	Total	24	36	24	26	36	4	25	121
		Urban	Deciduous	Redcedar	Ag Land	Rangeland	Wetland	Water	
	Producer's Accuracy (Omission)	96%	47%	79%	73%	47%	50%	96%	
	User's Accuracy (Commission)	92%	68%	76%	76%	68%	8%	96%	
	Overall Accuracy	69%							
	Kappa Statistic	64%							
Summer		Reference Data							
(August 1, 2011)		Urban	Deciduous	Redcedar	Ag Land	Rangeland	Wetland	Water	
Classification Data	Urban	25	0	0	0	0	0	0	25
	Deciduous	0	21	0	4	0	0	0	25
	Redcedar	0	4	17	0	1	1	2	25
	Ag Land	1	1	0	18	4	1	0	25
	Rangeland	2	2	1	1	18	1	0	25
	Wetland	2	11	0	0	0	7	5	25
	Water	2	0	0	0	0	2	21	25
	Total	32	39	18	23	23	12	28	127
		Urban	Deciduous	Redcedar	Ag Land	Rangeland	Wetland	Water	
	Producer's Accuracy (Omission)	78%	54%	94%	78%	78%	58%	75%	
	User's Accuracy (Commission)	100%	84%	68%	72%	72%	28%	84%	
	Overall Accuracy	73%							
	Kappa Statistic	68%							
Multi-date		Reference Data							
(Both Dates)		Urban	Deciduous	Redcedar	Ag Land	Rangeland	Wetland	Water	Total
Classification Data	Urban	25	0	0	0	0	0	0	25
	Deciduous	0	20	2	2	1	0	0	25
	Redcedar	0	0	25	0	0	0	0	25
	Ag Land	2	0	0	18	3	2	0	25
	Rangeland	0	2	0	1	22	0	0	25
	Wetland	0	13	0	1	1	8	2	25
	Water	1	0	0	0	0	1	23	25
	Total	28	35	27	22	27	11	25	141
		Urban	Deciduous	Redcedar	Ag Land	Rangeland	Wetland	Water	
	Producer's Accuracy (Omission)	89%	57%	93%	82%	81%	73%	92%	
	User's Accuracy (Commission)	100%	80%	100%	72%	88%	32%	92%	
	Overall Accuracy	81%							
	Kappa Statistic	77%							

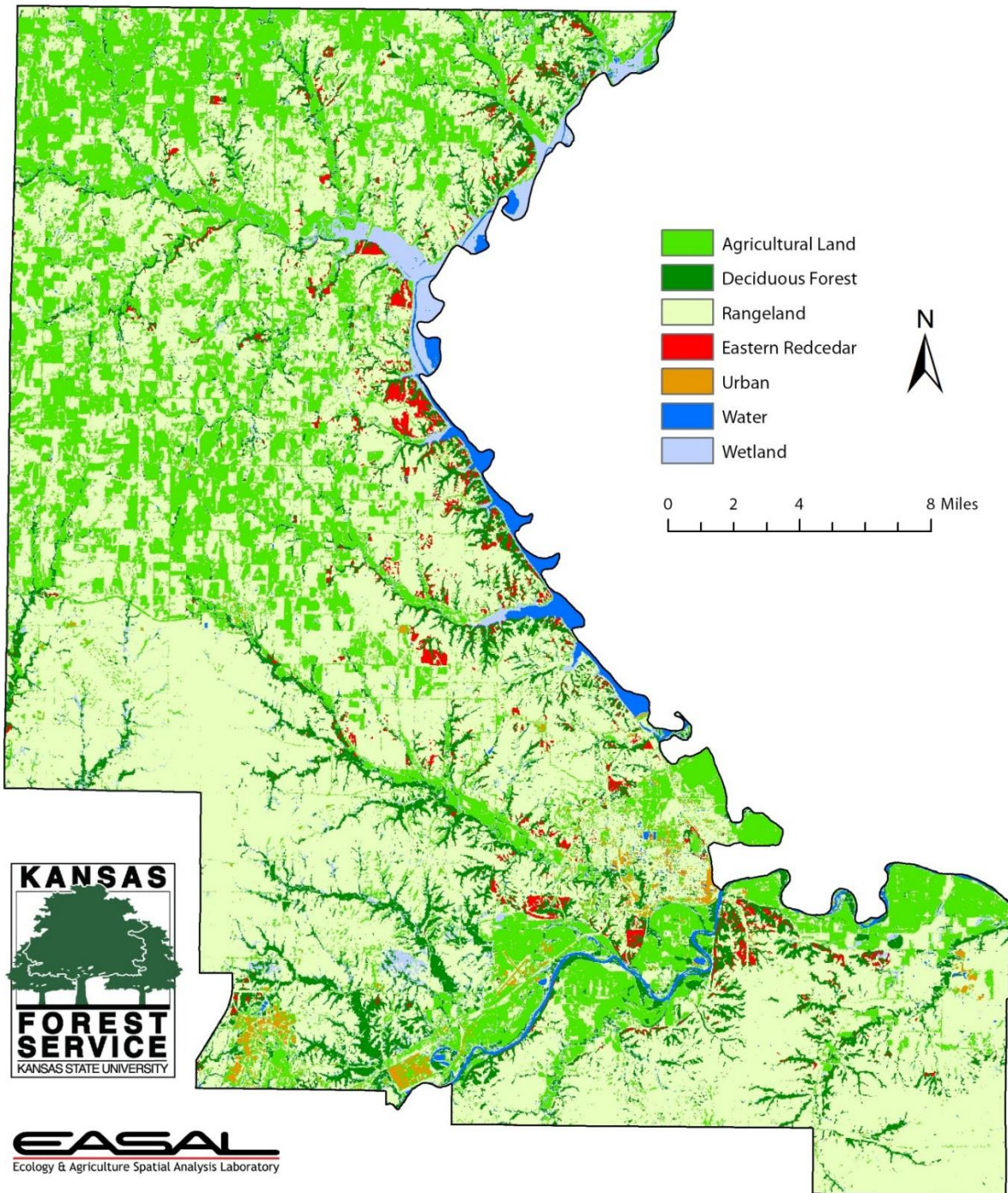


Figure 2.5 Multi-temporal Support Vector Machine (SVM) classification of Riley County, KS.

Discussion

The underlying assumption behind the multi-seasonal classification approach was that eastern redcedar cover would be confused with other photosynthetically-active vegetation cover types in a single-date classification. Redcedar is an evergreen species, so it retains photosynthetically-active leafy material throughout the year. It is therefore more spectrally stable than other land cover types that go into senescence during winter (*e.g.* summer crops, deciduous forest). Using multi-temporal data in this classification offered a way to separate redcedar cover from other land cover types that show greater spectral variation through the course of the year. Other studies showed varying degrees of success with multi-temporal classifications, and it was decided that it would be an appropriate method for this particular situation.

It was learned that the spectral properties of eastern redcedar caused it to be confused most often with shadowed areas (such as along steep stream banks), rather than other vegetation types in single-date classifications. This characteristic appears to be related to “microshadows” inherent in redcedar’s coniferous canopy structure that cause redcedar to appear spectrally darker than broadleaf trees (Figure 2.6). Classifying multi-temporal image datasets helped to account for the seasonal variability in spectral characteristics of each land cover type and also helped to distinguish between shadowed areas and redcedar cover.

SVM dramatically improved the accuracy of redcedar classifications over earlier attempts using traditional classifiers. Eastern redcedar cover represented a relatively small portion of the total classified area, making it more difficult to find redcedar training sites than it was for other cover types. SVM gave an accurate classification of eastern redcedar cover, despite the small number of training pixels provided. Another one of SVM’s strengths is its lack of assumptions about the normality of the data. The imagery we used showed a multi-modal histogram distribution because certain land cover types (*e.g.* water and rangeland) were more prominent than others. These characteristics of SVM allowed it to perform better than earlier attempts using supervised (Maximum Likelihood) and unsupervised (ISODATA) parametric classifiers.

It should be noted that the goal of the study was to accurately classify eastern redcedar cover, so overall classification accuracies were considered secondary in importance to accurate classification of redcedar cover. Of the two measures of redcedar classification accuracy (producer’s and user’s accuracies), the user’s accuracy was considered most important because it indicated the likelihood that redcedar would be present in a classified pixel, rather than the

likelihood of confusing redcedar with other cover types. We wanted to produce a map that accurately showed the locations of large, harvestable redcedar stands that are commercially viable. In our study area, the multi-seasonal SVM classification did this perfectly with a measured user's accuracy of 100%.



Figure 2.6 High-resolution (1-meter spatial resolution) false-color composite of a neighborhood in Manhattan, Kansas, showing spectral difference between Eastern redcedar cover and broadleaf deciduous tree cover in June 2012. Redcedar cover is outlined by a 30m (spatial resolution) multi-temporal Landsat classification (yellow). Note dark spectral characteristics of redcedar versus bright appearance of neighboring broadleaf tree cover. Image courtesy USDA NAIP program.

Conclusion

Multi-temporal classification using a Support Vector Machine classifier offered a marked improvement in accuracy over single-date summer and winter classifications. Using this classification scheme for separating eastern redcedar cover from other land cover types in Riley County, Kansas yielded high producer's and user's accuracies (93% and 100%, respectively).

Multi-temporal classification using SVM shows great potential for classifying eastern redcedar and other coniferous species. Future work would include expanding this method to other areas prone to redcedar encroachment, both in Kansas and in other parts of the Great Plains region.

Chapter 3 - Evaluation of Eastern Redcedar (*Juniperus virginiana*) Biomass in Eastern Kansas with a Small Unmanned Aircraft System (sUAS)

Introduction

In recent decades, woody tree invasion has become a serious problem in the tallgrass prairie region of Eastern Kansas (Bragg & Hulbert, 1976). Because of rapid human settlement, overgrazing, and fire suppression, woody species have invaded sites that were once healthy tallgrass prairies (Briggs, *et al.*, 2002). Among the most invasive of these woody species is *Juniperus virginiana*, commonly known as eastern redcedar (Figure 1.1).

Eastern redcedar is a pioneer invader species that will readily spread over a short period of time (Van Haverbeke & Read, 1976). Prior to European settlement in Kansas, woody species (including redcedar) were primarily located in stream bottoms (lowlands) in the Flint Hills region (Bragg & Hulbert, 1976). The Spanish explorer Coronado wrote in 1541 as he travelled through the region, “There is not any kind of wood in all these plains, away from the gullies and rivers, which are very few” (Bragg & Hulbert, 1976). Before settlement occurred in the region, as woody species would spread into upland areas, they were naturally controlled by periodic wildfires. Using dendrochronological dating methods, these fires have been shown to have burned on average every four years in the Flint Hills prior to European-American settlement (Allen & Palmer, 2011). Since humans settled the historic range of redcedar, they have fragmented the landscape, constructing artificial barriers to fire (primarily roads) that have halted the natural progression of prairie fires, allowing redcedar to expand its presence (Briggs, *et al.*, 2002). Poor land management and plantings of redcedar in windbreaks have further accelerated its spread (Owensby, *et al.*, 1973). These factors have caused redcedar to become established in upland tallgrass prairies.

Redcedar’s invasiveness has become a problem in the Flint Hills region in north-central Kansas where many absentee landowners have acquired land as an investment or for hunting (Kindscher & Scott, 1997). These landowners may often be unwilling or unable to take the necessary steps—such as conducting annual prairie burns—to properly manage their property. As redcedar has spread into the uplands due to a lack of fire to control it, it has often turned into

dense stands which crowd out warm-season (C_4) native tallgrass prairie grasses and forbs (Gehring & Bragg, 1992). Many of these species are important forage plants for grazing animals in Kansas. Valuable rangelands can be converted into closed-canopy redcedar stands in as little as 40 years (Briggs, *et al.*, 2002). Beef cattle ranching is an important industry in Kansas, representing \$8.5 billion out of the \$14.4 billion agricultural industry in the state (USDA, 2011), and this industry is being threatened by the spread of redcedar into rangelands.

Another major concern with redcedar is its encroachment into populated areas. Redcedar foliage contains flammable volatile oils, and dense stands of redcedar located in urban and suburban areas can increase the risk of a wildfire affecting built-up areas (Ward, 2013).

Despite its invasiveness, eastern redcedar has been shown to be a useful species in industry and agriculture. It is commonly harvested for construction of pencils and wood chests, and it is also chipped into mulch for use in landscaping and gardening (Van Haverbeke & Read, 1976). Redcedar oil has also been extracted for use in the essential oil industry (Gawde, *et al.*, 2009; CAFNRnews, 2008; Semen & Hizirolu, 2005). It has also been shown to contain a high amount of energy for heating. Large individual trees have been shown to contain over twelve million British Thermal Units (BTUs) of energy, equivalent to around 106 gallons of heating oil, or 0.6 tons of anthracite coal (Strauss, *et al.*, 2011; Slusher, 1995). It has been proposed that redcedar could be harvested for use as a biofuel, providing an inexpensive, locally-obtained fuel source for Kansas. Redcedar wood can be converted into biodiesel, wood chips for wood burning boilers, or “biochar,” a charcoal soil amendment (Teel, 2012; Starks, *et al.*, 2011).

To promote a redcedar biomass harvesting industry, accurate surveys of redcedar stands are needed to estimate available biomass. An understanding of the allometric relationships between various plant metrics (diameter at breast height, canopy area, and height) and total aboveground biomass allows for accurate redcedar biomass estimates when ground measurements are performed. These allometric relationships have been detailed in multiple studies involving eastern redcedar and other juniper species (Norris, *et al.*, 2001; Starks, *et al.*, 2011; Strauss, *et al.*, 2011; Ansley, *et al.*, 2012). Total aboveground biomass can be used to calculate the British Thermal Unit (BTU) potential of the trees (Strauss, *et al.*, 2011, Slusher, 1995)

Remote Sensing with sUAS

sUAS have gained popularity in recent years in a wide variety of applications in the environmental sciences. Rangeland monitoring and grassland species mapping, including classification of invasive species, have been performed extensively using aerial imagery from sUAS (Laliberte, *et al.*, 2010; Hardin & Jackson, 2005; Hardin, *et al.*, 2007). sUAS have also been utilized for remote sensing of forested lands (Wing, *et al.*, 2013), although no studies were found that utilized sUAS for remote sensing of eastern redcedar.

An sUAS offers several advantages over traditional aerial photography platforms (satellites and manned aircraft). First, recent advancements in technology are allowing sUAS components (autopilot, receiver, *etc.*) to cost less than ever before, allowing unmanned aircraft to be a viable low-cost solution for remote sensing. Second, sUAS are typically flown at low altitudes (< 200 m), enabling ultra-high resolution imagery to be collected. This imagery can be of extremely high detail, allowing for analysis of features that would not be visible in coarser spatial resolution imagery. The low altitudes at which sUAS are flown also help to mitigate the effects of the atmosphere on remotely sensed data. Third, sUAS are easily deployable, meaning that they can be flown by a trained user at a desired location whenever weather conditions are suitable, without relying upon the availability of a manned airplane and professional pilot. Fourth, they can be programmed to fly imagery of exactly the same location on a repeatable basis, such as during different periods of the growing season, to offer multi-temporal imaging capability. In this study, the nature of the problem—accurately measuring canopy area of individual redcedar trees—required very high spatial resolution (<0.5 m pixel size), making sUAS an ideal aerial photography platform for detecting redcedar.

The goals of this study were to:

- 1) Measure the canopy area of individual redcedar trees that are encroaching into a tallgrass prairie in order to estimate their total aboveground biomass using aerial imagery from an sUAS.
- 2) Establish a simple workflow that can be used for rapid acquisition of ultra-high spatial resolution aerial imagery over a relatively small area (260 ha imaged in 20 minutes of flight time) using an sUAS. This workflow can be effective for evaluating trees from the air in an automated fashion, avoiding the cost and inefficiency of extensive ground surveys.

Methods

Study Area and Ground Reference Data Collection

The study area was located six kilometers SE of Manhattan, Kansas at the Rannells Flint Hills Tallgrass Prairie Preserve (39.136°, -96.532°). The Rannells Preserve is a rangeland research area managed by Kansas State University to test various grazing and burning regimes and their impacts on the tallgrass prairie ecosystem. This site was chosen because of the presence of redcedar trees expanding into an upland area from a stream bottom, as well as the availability of a certificate of authorization (COA) from the Federal Aviation Administration (FAA) allowing us to fly a sUAS in this location. The site is located in the Flint Hills region of Kansas, and therefore contains steep, rocky topography. The elevation of the study area ranged between 370 m and 420 m. Common grasses at the site include big bluestem (*Andropogon gerardii*), indiagrass (*Sorghastrum nutans*), little bluestem (*Andropogon scoparius*), and Kentucky bluegrass (*Poa pratensis*). Perennial forbs are also common at the site, including ironweed (*Veronia baldwinii*), western ragweed (*Ambrosia psilostachya*), white sagebrush (*Artemisia ludoviciana*), and slim flower scurfpea (*Psoralea tenuiflora*) (Owensby, 2014). Trees are present in the lowland portions of the site, such as osageorange (*Maclura pomifera*) and the species of interest, eastern redcedar.

Prior to the flight, 14 redcedar trees across a broad size gradient were measured and weighed in various locations around Manhattan, Kansas to verify the allometric relationships between various tree measurements (canopy area, diameter at breast height, and height) and biomass. We found a strong relationship between canopy area and total aboveground biomass ($r^2 = 0.90$) (Figure 3.1). The resulting regression equation was used to calculate the biomass of each redcedar in the study area based upon its canopy area.

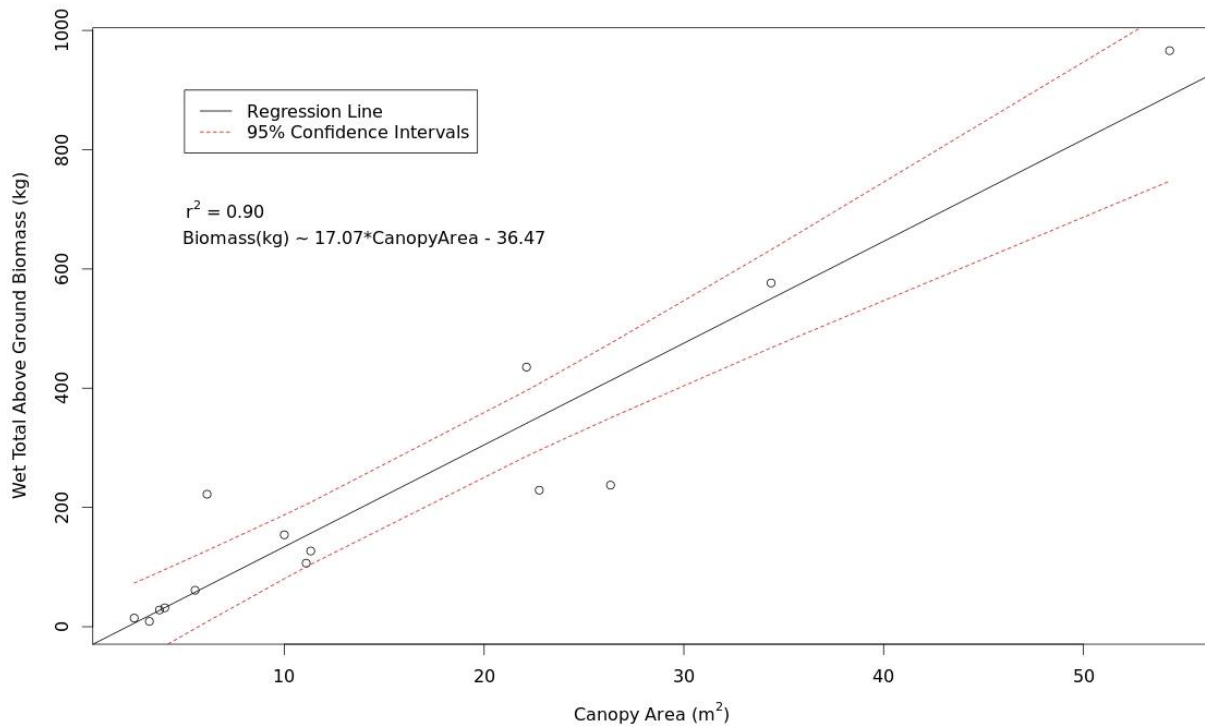


Figure 3.1 Graph showing the allometric relationship between redcedar canopy area (m²) and wet total aboveground biomass (kg). The resulting regression equation is also shown.

Flight Preparation

Prior to the flight, permission was requested from the Federal Aviation Administration (FAA) to operate an sUAS at the study location. The FAA granted permission in the form of a COA, which stipulates that the unmanned aircraft must be flown under the following restrictions:

- Altitude must not exceed 400 feet (122 meters) above ground level (AGL)
- A “pilot in command” must be present who is a licensed pilot
- The aircraft may not approach within five miles of the nearest airport
- The aircraft must be flown via line-of-sight, *i.e.* the pilot must be able to see the aircraft at all times with the unaided eye and direct it to avoid obstacles
- Contact must be made with the nearest airport control tower to advise them of sUAS operations in the area

Our sUAS flight team included a licensed pilot, and we followed each of these requirements as we performed this study. The nearest controlled airport (KMHK) was notified at the start and conclusion of the flight.

Zephyr II sUAS

The imagery was flown on August 7, 2013 using a Ritewing© Zephyr II platform paired with an ArduPilotMega (APM) 2.5 autopilot system (Figure 3.2), operated with firmware version 2.73. This platform is a 54-inch wingspan delta wing design, constructed with lightweight EPOR foam. The platform was custom-built from a kit sold by the manufacturer. A hole was cut in the center of the airframe in order to mount a downward-facing color infrared camera for nadir imaging. The platform is hand-launched and lands on its belly, preferably on a soft, flat, grassy strip. The total weight of the Zephyr II, including electronic components and imaging sensors, is around 2.3kg.

The APM 2.5 system is an inexpensive, open-source autopilot solution that allows the user to adjust all flight parameters and to program repeatable waypoints for a given mission using the APM Mission Planner software package. This capability was utilized in this study to set up 10 flightlines to achieve complete coverage (50% sidelap) over the study area and maintain a constant altitude of 122 meters above ground level (the maximum allowed by the COA, and greater than the altitude necessary to achieve 50% forward overlap between images). A laptop computer was used as a ground station in the field to monitor the progress of the mission and the status of flight parameters. A series of waypoints were programmed using the ground station software to achieve complete coverage of the study area. The APM Mission Planner ground station software communicates with the APM autopilot system via a 915 MHz telemetry data link. Direct and redundant control was provided through a 2.4 GHz transceiver radio control system. To initiate autopilot control, the APM is powered up and monitored until a GPS signal is acquired. The aircraft is hand-launched and manually piloted via radio control. Next, the autopilot is activated, and the system guides the aircraft to a series of consecutive waypoints. When the aircraft has finished flying to each waypoint, it is programmed to return to “home,” or the coordinates where the APM initially achieved a GPS lock, and circle overhead. Finally, the pilot deactivates the autopilot and manually lands the aircraft.



Figure 3.2 UAS pilot (Dr. Deon van der Merwe) preparing the Ritewing Zephyr II sUAS for flight. Photograph courtesy of Joel Prince.

Sensors

A modified Canon PowerShot S100 12.1 MP digital camera was used to image the study area. The camera was modified by LDP, LLC© (Carlstadt, New Jersey, USA) to record images in near-infrared, green, and blue wavelengths. These wavelengths are desirable for calculating vegetation indices and for differentiating between vegetated and non-vegetated land cover types.

Redcedar trees were easily distinguishable from other tree species in the imagery due to their low reflectance in the near-infrared wavelengths compared to deciduous trees (Figure 3.3). Images were captured in the camera's RAW+JPEG mode, using fixed shutter speed, aperture, and ISO settings (1/2000 second, f/2, ISO-200) We used the Canon Hack Developer's Kit (CHDK) intervalometer script to trigger the camera's shutter at 3.5-second intervals during flight

(the fastest interval possible for this camera model). A forward-looking GoPro HD Hero2 video camera was also used to acquire high definition video footage of the flight (Figure 3.4).

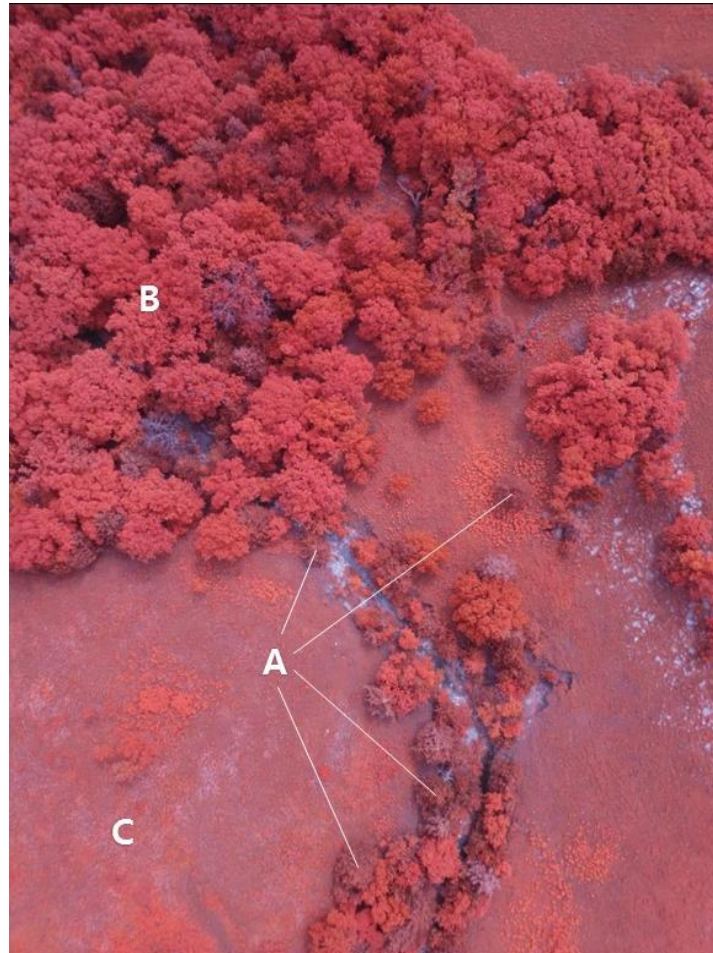


Figure 3.3 Sample color-infrared image taken by the Canon PowerShot S100 camera over the study area showing redcedar trees (A), deciduous forest (B), and tallgrass prairie areas (C).



Figure 3.4 Video frame from the GoPro HD Hero2 video camera taken over the study area.

Image Processing

196 useable images were captured with the PowerShot S100 during the flight. A few images were considered unusable due to blurriness or an oblique viewing angle when the shutter trigger occurred during banked turns. These images were excluded from the final mosaic. After collecting the images, it was decided that the lower-quality JPEG format was suitable for the project because there was not a need for precise spectral measurements in this study. RAW format images contain “pure” sensor data that has not been compressed, but they are much larger in size than their JPEG counterparts. RAW images are generally recorded by the camera in a brand-specific proprietary format (*e.g.* Canon .CR2 format) that needs to be converted to a generic format (such as TIFF) for analysis in most image processing software packages. This requires extra time and computer processing power that were deemed unnecessary to achieve the goals of this study.

The useable JPEG images were geometrically corrected for lens barrel distortion using Canon Digital Photo Professional software, and mosaicked using Agisoft Photoscan Professional. This software package uses a photogrammetric splicing algorithm to automatically

stitch the images into a seamless orthophoto mosaic. As the images are stitched together, the algorithm averages the pixel values for a given location using the values from each individual image that contains that location (Figure 3.5). The mosaic process required several hours of computer processing time.

After the mosaic was completed, ESRI ArcGIS 10.1© was used to georegister the orthomosaic. Total RMS error was 0.36 meters. Individual redcedar trees were then identified based upon knowledge of the study area, as well as the trees' darker appearance in the imagery versus deciduous species. These trees' canopies were digitized as polygon features and their areas were calculated using the field calculator tool in ArcGIS (Figure 3.6).

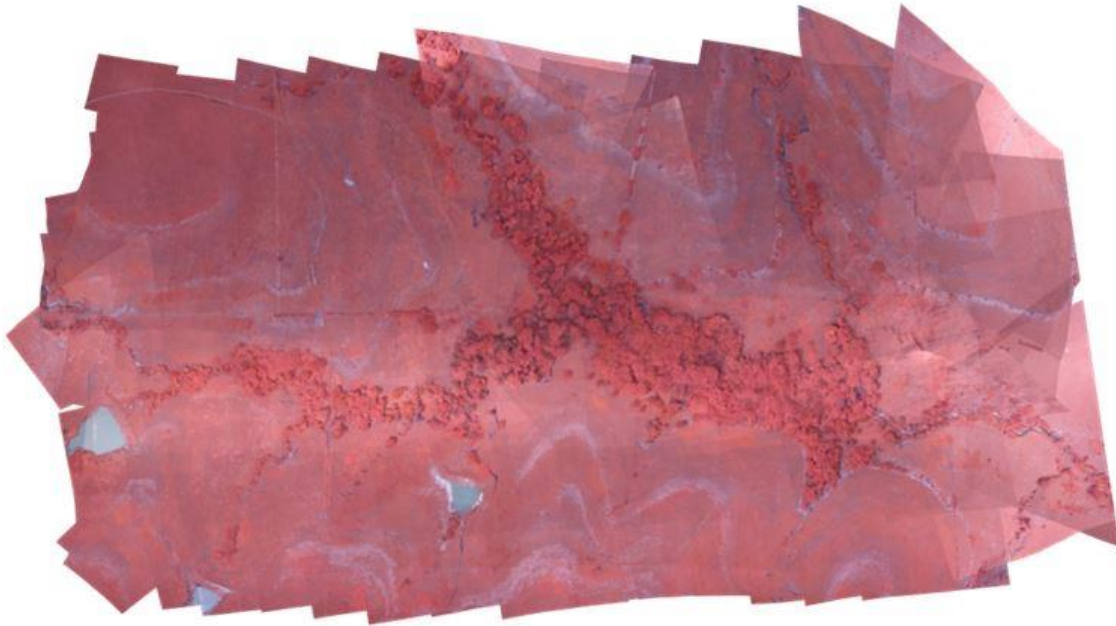


Figure 3.5 Orthophoto mosaic of the study area produced by Agisoft Photoscan Professional software. This mosaic incorporates data from approximately 180 individual images that represented approximately 93 ha of ground area. Note the presence of seamlines in portion of the mosaic caused by variable cloud conditions.

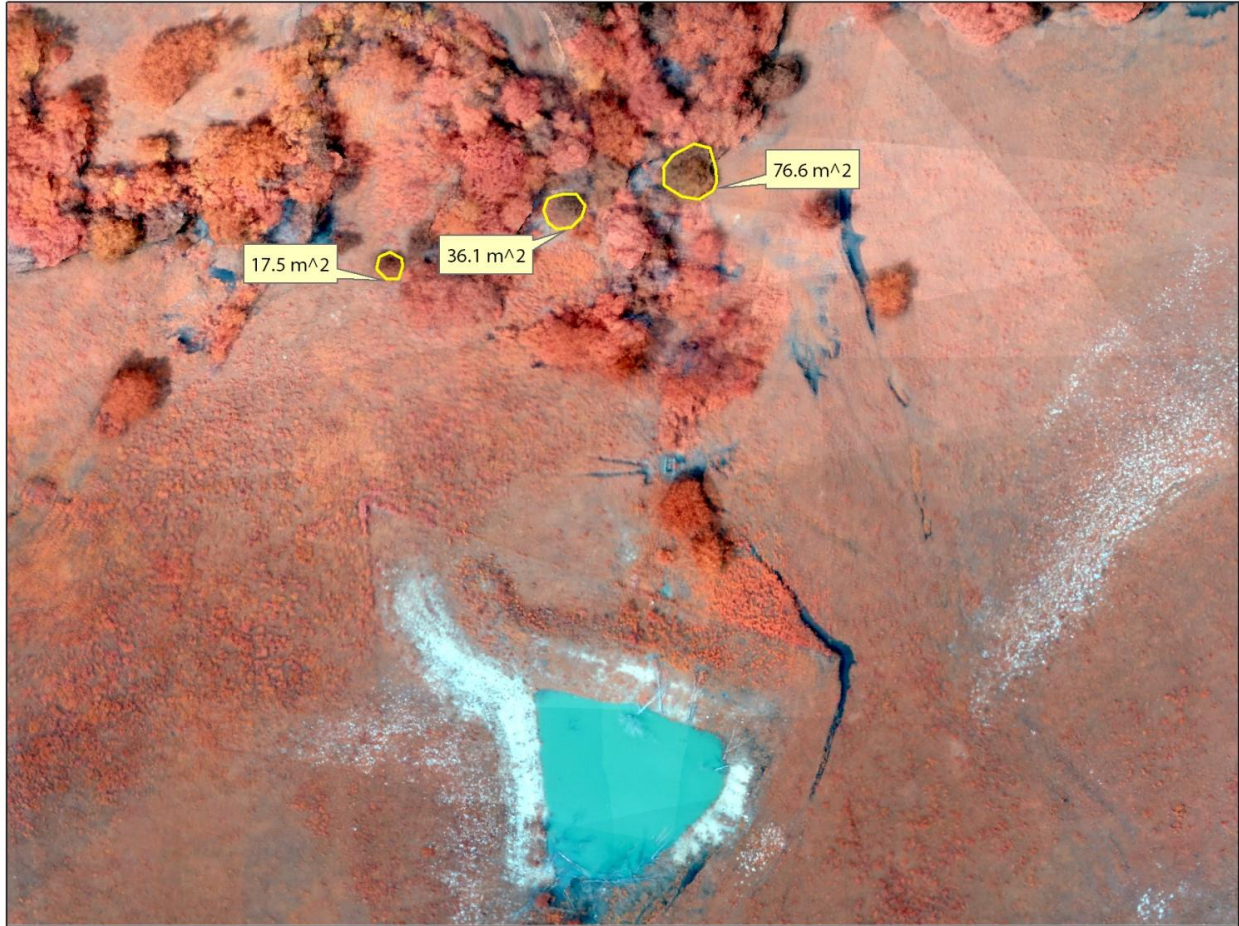


Figure 3.6 Polygons are drawn around the canopy of each redcedar to measure their canopy area using ArcGIS software.

Discussion

The strength of the correlation between canopy area and total aboveground biomass indicated that aerial measurement of canopy area using high resolution orthorectified imagery acquired using an unmanned aerial vehicle is a reliable means of estimating redcedar biomass. This approach is limited, however, to situations where individual trees are growing apart from other trees. When trees have grown together into a coalescing stand, this method will no longer be appropriate. In a situation where the canopies of multiple trees have coalesced, a model should be developed where some other measurement is used to predict biomass (e.g. percent cover).

The secondary goal of this study was to perform a proof of concept to determine if imagery from a small unmanned aircraft would be useful for quantifying redcedar biomass. We

developed a workflow (Figure 3.7) for acquiring imagery that we found to be simple and fast, and it is a workflow that could be used for a multitude of applications when accurate ground measurements are needed.

sUAS Remote Sensing Workflow

1. Site Reconnaissance	Identify a suitable site where the phenomenon of interest is present through ground surveys and/or analysis of existing aerial imagery
2. Acquire and Prepare Platform and Sensors	Determine which platforms (e.g. multirotor, fixed-wing) and sensors (e.g. multispectral, thermal) would be most suitable for safely detecting the phenomenon of interest. Thoroughly test the platform and sensor together to ensure reliability
3. FAA COA Application	Submit COA application for the area of interest.
4. Overflight	Once COA is received, plan and execute overflight as specified in the COA
5. Post-Processing of Image Data	Manually examine images to remove blurry or oblique images; input usable images into mosaic software (e.g. Agisoft Photoscan Professional) to produce orthomosaic; georegister orthomosaic using GIS software
6. Analyze and Interpret Results	Perform analysis of phenomenon of interest using GIS and/or image analysis software

Figure 3.7. sUAS remote sensing workflow used in this project.

Future work would include improving the canopy area versus biomass allometric equation so it works well across a larger area (e.g. at the state or regional level). This would require measuring and weighing trees along a biomass gradient across the region of interest. If the proper allometric models are developed for different regions, this method could be utilized to rapidly estimate the biofuel potential of invading trees in any area of concern.

Chapter 4 - Assessment of Eastern Redcedar (*Juniperus virginiana*) Biomass Using LiDAR and Multispectral Imagery

Introduction

For over 50 years, the invasion of woody plant species into rangelands throughout the tallgrass prairie ecoregion has been a serious concern to ranchers and conservationists (Owensby, *et al.*, 1973). Among the most prominent of these species is *Juniperus virginiana* L., often called eastern redcedar (Owensby, *et al.*, 1973; Norris, *et al.*, 2001) (Figure 4.1). Eastern redcedar has a large range encompassing most of the eastern United States. (Norris, *et al.*, 2001) The species is fast-growing, and birds can transport its seeds over many miles (Briggs, *et al.*, 2002). Historically, prior to the widespread suppression of natural prairie fires in the region, periodic burning of the prairie prevented eastern redcedar overexpansion (Briggs and Gibson, 1992; Briggs, *et al.*, 2002). Anthropogenic fire suppression has now resulted in the drastic expansion of its range (Strine, 2004; Owensby, *et al.*, 1973). This expansion has become an economic threat to the cattle ranching industry due to the loss of rangeland available for cattle grazing in much of the Great Plains (Schmidt, 2002). Along with economic impacts caused by redcedar expansion, there are also environmental impacts, including losses in plant and animal community diversity (Chapman, 2004; Horncastle, 2005; Briggs, *et al.*, 2002). Closed-canopy redcedar forests also present a wildfire danger where redcedar expansion occurs near urban areas (Ward, 2013).

A potential solution to the problem of redcedar invasion is to find a large-scale commercial use for redcedar biomass. Since eastern redcedar is a plentiful species that is “out of place” (Blatchley, 1912) in the prairie ecosystem, there has been interest in harvesting redcedar stands for a variety of uses. Traditionally, redcedar wood has been used in fence posts and furniture, and it is commonly turned into mulch for gardening use. The wood can also be chipped and burned in wood-burning stoves or boilers, and methods are being developed to convert redcedar material into liquid biofuel products (Hemmerly, 1970; Lam, 2012; Ramachandriya, *et al.*, 2013). Redcedar oil has also been utilized in the essential oil industry and reportedly has antibacterial and anti-cancer properties (Gawde, *et al.*, 2009; CAFNRnews, 2008; Semen & Hiziroglu, 2005).



Figure 4.1 Eastern redcedar in Riley County, Kansas.

Before redcedar can be harvested for use as a biofuel or other product, it must be determined if there is enough redcedar biomass in an area to allow a harvesting industry to be economically viable in that area, especially considering the costs of transporting the trees from harvest locations to a refinery. In order for harvesting to be cost-effective, it is best that large numbers of trees be clustered tightly together within an economically sustainable distance of processing facilities. While estimates of the overall scope of redcedar invasion and general estimates of biomass exist (Grabow and Price, 2010; Moser, *et al.*, 2008), there is little information on the spatial distribution of this biomass within Kansas. The existing biomass information was collected using a random ground sampling technique (Bechtold & Patterson, 2005), and has been shown in many cases to be inaccurate at a county level.

In light of eastern redcedar's detrimental environmental and economic impacts, as well as its potential commercial benefits, the major objectives of this project were to:

- 1) Establish an allometric equation using various plant metrics (diameter at breast height and tree height) to predict redcedar biomass at the individual tree and study plot (225m²) levels.
- 2) Use LiDAR imagery, along with multispectral image data, to classify redcedar stands across a large area (*e.g.* county) and estimate redcedar biomass across that area.

Use of LiDAR and multispectral imagery in forest inventories

While there are general volumetric and areal estimations of redcedar invasion, there is little information on the exact spatial extent and density of biomass. In order to determine the cost benefit of redcedar harvest, there must be accurate estimates of standing biomass within areas under consideration for harvest operations. Multispectral imagery has been used in the past to assess redcedar extent and biomass. Wylie *et al.* (2000) used Airborne Visible/Infrared Imaging Spectrometer (AVIRIS) data to map eastern redcedar in the Nebraska sand hills. Starks, *et al.* (2011) found a strong correlation between derived metrics from high-resolution satellite imagery (0.42 m/pixel) and aboveground redcedar biomass.

In addition, studies have shown that Light Detection and Ranging (LiDAR) is a powerful tool for assessing forest biomass due to its ability to generate multiple returns (height measurements) within a single pulse when that pulse penetrates gaps in tree canopy (Figure 4.2). As a result, LiDAR data have been used extensively in surveys of native or highly managed forest stands. In 2003, Drake, *et al.* conducted a study where plot-level mean height of median energy derived from waveform LiDAR was combined with a linear regression technique to model aboveground biomass in neo-tropical forest. Popescu and Wynne (2004a) utilized a method of individual tree extraction based on a local maxima variable window approach. This method also utilized spectral data to differentiate between coniferous trees and deciduous trees when calculating window size based on a canopy-size-to-height ratio of the two tree types. In 2005, Bortolot and Wynne used an individual tree-based approach to estimate the biomass of a forest in Virginia. These studies all focused on either estimating biomass of single species in homogenous forest, or estimation of total aboveground biomass within a heterogeneous forest. When an estimate of the biomass of a single tree species within a heterogeneous area is

necessary, it becomes advantageous to combine LiDAR with multispectral imagery to differentiate biomass of different species. Recently, multiple attempts have been made to use LiDAR in conjunction with multispectral or hyperspectral imagery to map the biomass of invasive woody species in a mixed landscape. Swatantran, *et al.* (2011) found that incorporating hyperspectral classification improved their ability to predict biomass of a specific species when using waveform LiDAR in the Sierra Nevada. Another study utilized a data fusion of LiDAR and leaf-off ATLAS imagery to improve the performance of individual tree delineation and biomass estimation of deciduous and coniferous trees (Popescu & Wynne 2004b). These studies showed that the fusion of LiDAR and multispectral imagery can be beneficial for accurate biomass estimation of target species and tree types.

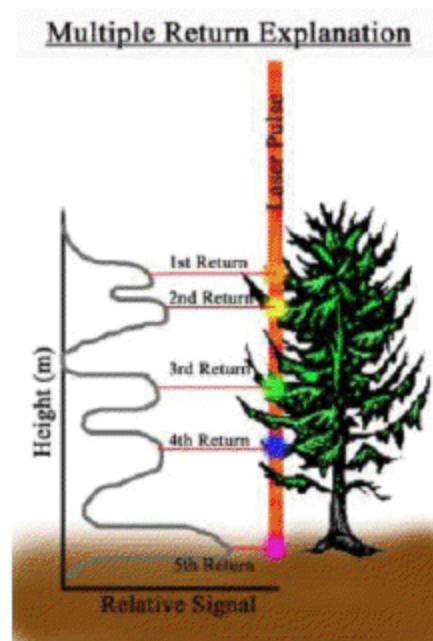


Figure 4.2 Illustration of multiple returns from a LiDAR pulse within a tree canopy. From Stoker (date unknown).

For this project, we used a plot-based regression technique utilizing LiDAR-derived canopy height, together with a classification derived from multispectral data, rather than an individual tree-based approach. The reasons for this hybrid methodology include the relatively sparse point spacing of the available LiDAR data (1.4 meters) and the variable nature of redcedar tree crown shape. Window size calculations necessary for individual tree extraction require

knowledge of crown structure and differ by tree species. Redcedar trees can show a wide variety of crown structures (*e.g.* conic or columnar), making individual tree extraction problematic when attempted over large areas.

Methods

Study Area

The project study area, Riley County, Kansas, was identified by the Kansas Forest Service as a county of concern due to its high rate of redcedar encroachment. An unpublished study estimated a 23,000% increase of redcedar cover in Riley County between 1965 and 2005 (Grabow & Price, 2010). Riley County lies within the Flint Hills ecoregion. Portions of the county are topographically rugged, with steep stream banks punctuating rocky upland areas. The native vegetation consists of tallgrass prairie species—primarily big bluestem (*Andropogon gerardii*), indiangrass (*Sorghastrum nutans*), and little bluestem (*Andropogon scoparius*)—in the uplands. Trees, including hackberry (*Celtis occidentalis*), American elm (*Ulmus americana*), green ash (*Fraxinus pennsylvanica*), and black walnut (*Juglans nigra*) are found along the stream bottoms (Owensby, 2014). The elevation ranges from 298 meters in the Kansas River Valley to 464 meters in the west-central portion of the county. Tuttle Creek Reservoir (along the Big Blue River) is a dominant feature in the county. Manhattan, the county seat and home of Kansas State University, is the largest city. The total area of the county is 1611 km² (U.S. Census Bureau, 2013), the majority of which is utilized for cattle grazing and crop production. The climate in Riley County is classified as humid continental (Köppen *Dfa*) (Peel, *et al.*, 2007).

Collection of in situ ground reference data

Our data collection, image classification, and biomass assessment workflow is outlined in Figure 4.3. We collected *in situ* data in seventeen ground reference plots throughout Riley County, Kansas across a redcedar cover and biomass gradient (Figure 4.4). Plots were approximately 15 by 15 meters for an approximate total area of 225 m² per plot. A GPS position was collected for the center of each plot and the four corners were measured out and situated at NE, NW, SE, and SW compass directions. The plots were digitized in ArcGIS® to facilitate extraction of percent cover metrics (derived from classification of multispectral imagery) and height metrics derived from LiDAR for each plot.

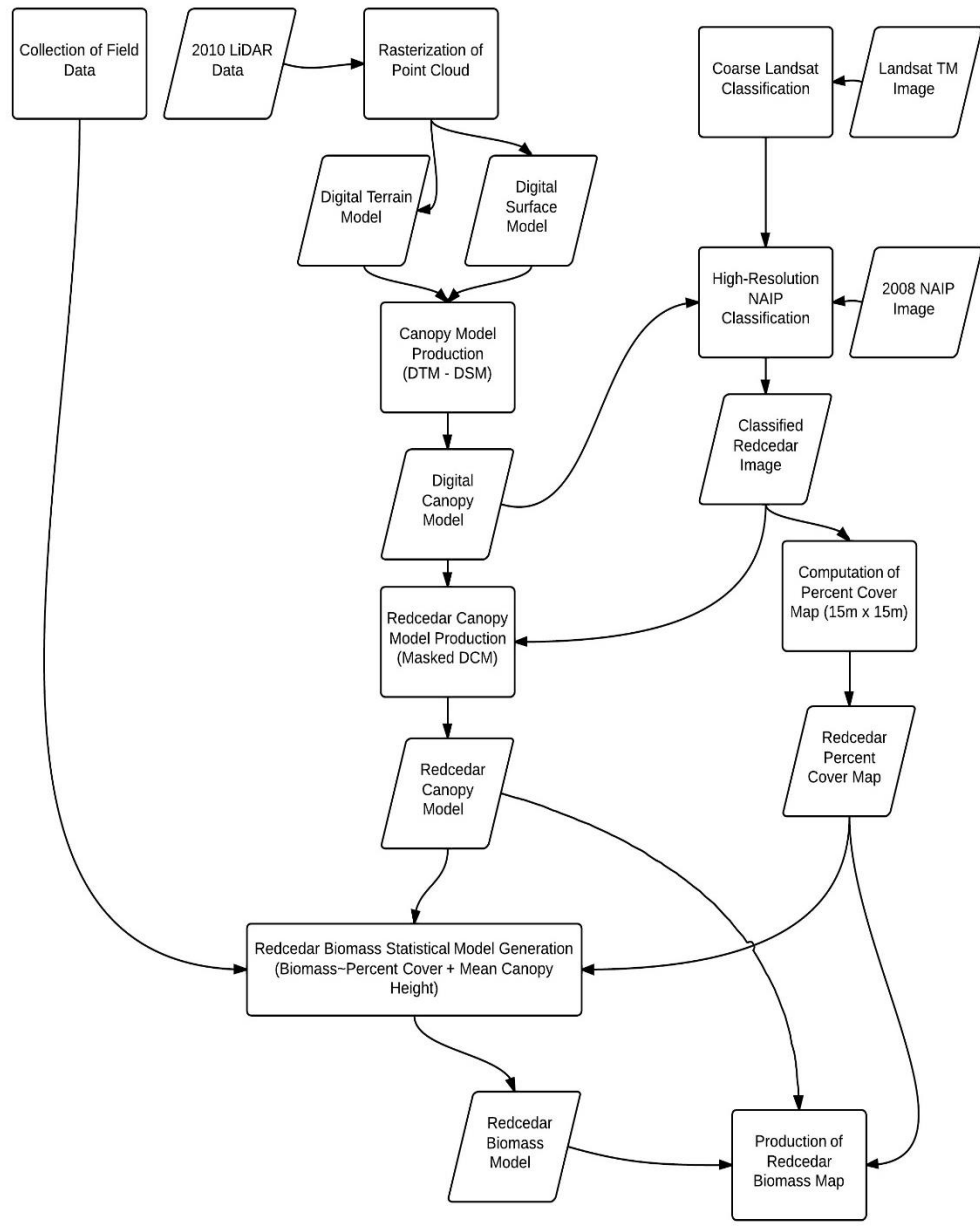


Figure 4.3 Redcedar classification and biomass mapping workflow.

Biomass was estimated for each tree within the plot using diameter at breast height (DBH) as an input into an allometric equation based on our own data and data collected by the students of the Kansas State University Natural Resources and Environmental Sciences capstone course. DBH has been found to be a reliable predictor of individual tree total aboveground biomass when it is not possible to weigh each tree (Figure 4.5)—a similar equation was used by

Norris, *et al.* (2001) to estimate redcedar biomass. Total biomass estimates for each plot were calculated by summing the estimated biomass of every tree with a DBH of greater than two inches. The two-inch threshold was chosen because trees with DBH smaller than two inches were considered to have negligible biomass from a harvest standpoint and were also considered too small to be easily detectable in the aerial image data used in this project (1-meter spatial resolution). Age and height estimates of five trees in each plot were also collected to further characterize the sites and for validation of remotely sensed height models. These trees were selected using a modified point-center quarter method, where the tree closest to the center point and each of the four midpoints between the center and the four corners of the sample site was selected for height and tree age estimation (Mitchell, 2010) (Figure 4.6). Height was calculated using a clinometer, and tree age was estimated for some sites by taking core samples using an increment borer. (It was quickly realized that tree age would not improve biomass prediction, so average ages were not calculated for all sites.) Canopy density was measured using a densiometer facing each of the four cardinal directions from each of these points. Densiometer measurements were averaged for each site and used to help validate remotely sensed percent cover estimates. Site characteristics are summarized in Table 4.1.

Table 4.1 Summary of site measurements for each ground reference plot.

Site	Average Age	Max Age	LiDAR Derived Canopy Height (m)	Ground Mean Tree Height (m)	Percent Cover Derived From Imagery	Densiometer Cover	Biomass (kg)
1	34.6	45	6.096	8.33	81.43%	92.24%	4992.73
2	30.25	40	2.902	7.70	46.94%	61.10%	2936.36
3	37	48	4.032	7.97	80.89%	81.44%	5288.64
4	29	43	2.76	7.91	50.00%	37.28%	3506.36
5	24	28	1.939	4.73	59.18%	42.22%	1595.00
6	N/A	N/A	4.335	8.42	79.59%	99.32%	3492.73
7	N/A	N/A	3.712	7.71	78.57%	86.84%	6008.64
8	N/A	N/A	4.112	7.45	53.57%	98.28%	5667.27
9	N/A	N/A	1.828	7.23	48.47%	61.20%	1955.91
10	N/A	N/A	0.911	4.61	16.84%	11.13%	686.82
11	N/A	N/A	0.919	4.05	17.86%	8.68%	410.45
12	N/A	N/A	2.063	6.24	47.96%	50.80%	2122.27
13	N/A	N/A	5.845	N/A	79.59%	89.39%	6467.73
14	N/A	N/A	2.669	5.60	54.08%	68.07%	2555.91
15	N/A	N/A	5.372	7.75	63.27%	75.30%	3670.00
16	N/A	N/A	1.1	4.42	11.73%	10.24%	395.91
17	N/A	N/A	1.699	4.76	22.45%	8.32%	859.09

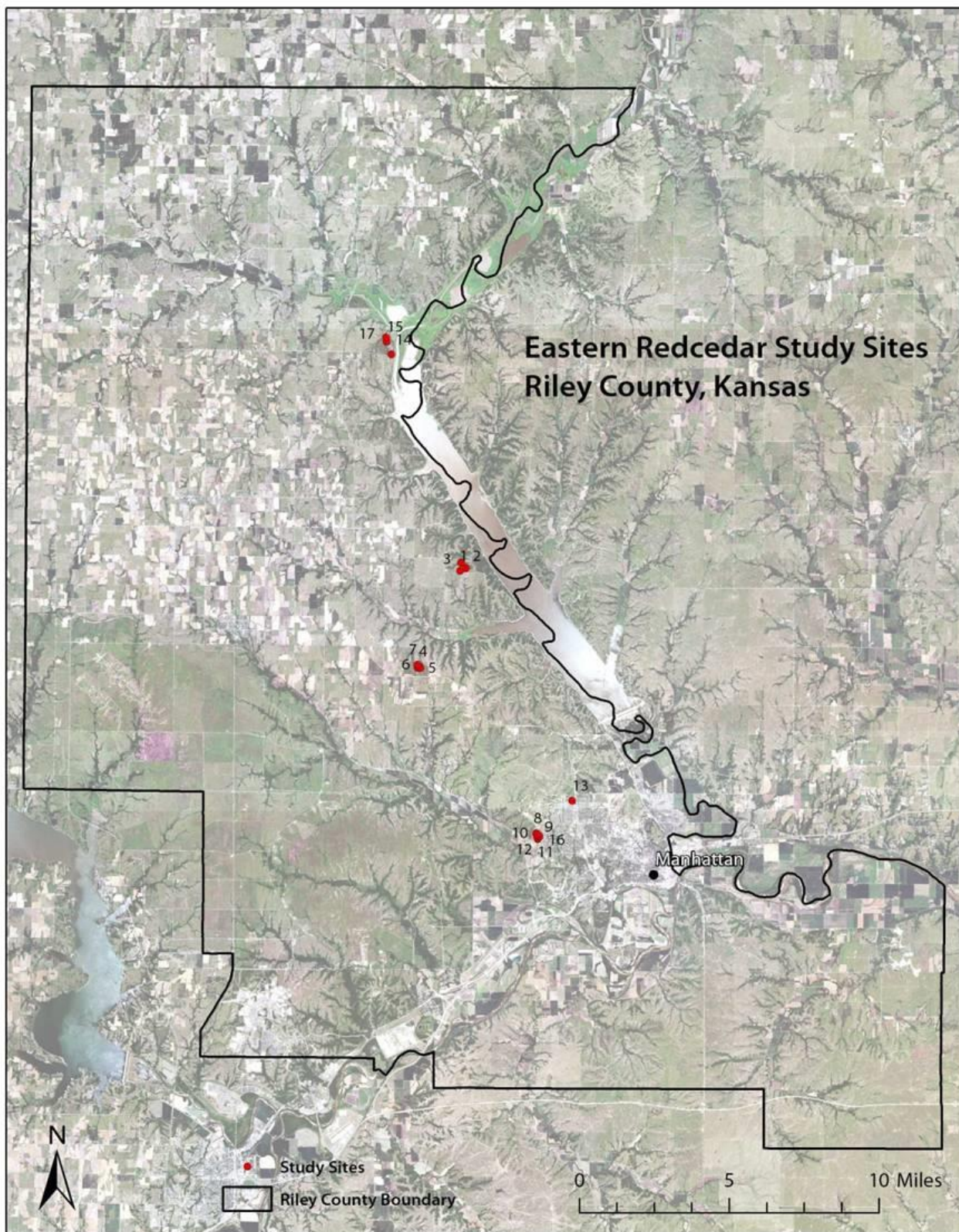


Figure 4.4 Map of Riley County, Kansas showing study plot locations.

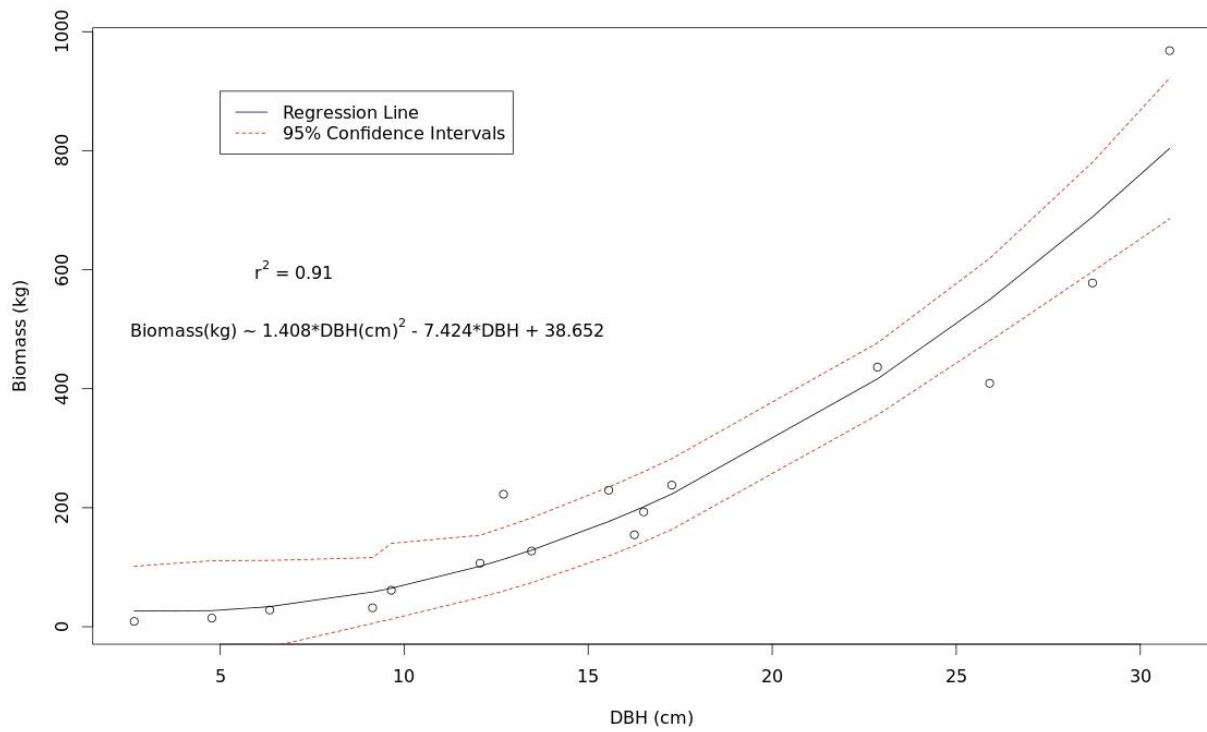


Figure 4.5 Allometric equation relating diameter at breast height (DBH) to biomass.

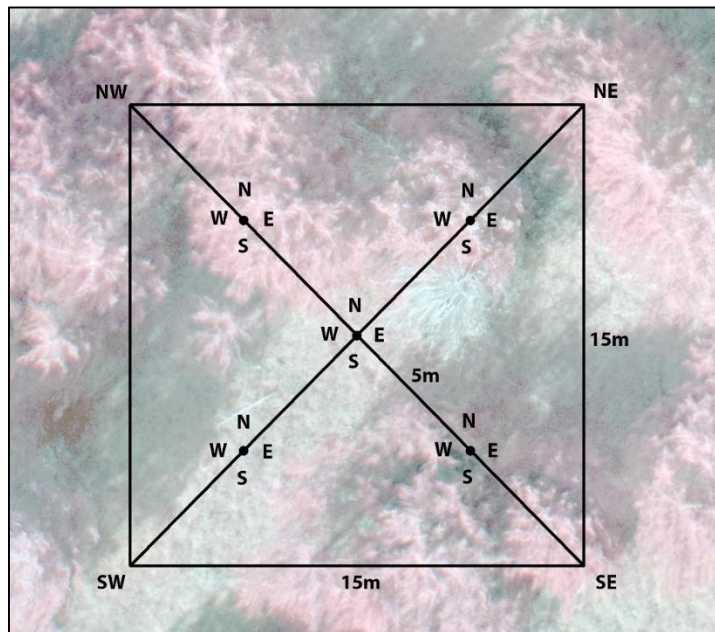


Figure 4.6 Aerial schematic of the modified point-center quarter sampling method at a study site.

LiDAR pre-processing

LiDAR data were obtained from the Kansas GIS Data Access Support Center (DASC) in raw .LAS format. The LiDAR data were collected in spring of 2010. Nominal point spacing was between 1 and 1.4 meters and vertical error was less than 18 centimeters. The distributor had classified ground returns within the dataset, but no further classification had been performed.

LiDAR LAS files were processed using the Merrick® Advanced Remote Sensing software package (MARS®), provided to us for temporary use by Merrick, Inc. The MARS® software allows several different methods for raster interpolation from an LAS point cloud (Merrick and Company 2013). One method interpolates raster cell values from a triangulated representation of the point cloud generated as an intermediary. Due to time constraints, this computationally intensive method was deemed impractical. The other method uses a binning process to assign grid cell values from point values: when more than one value is present, the software allows the user to select whether to use a minimum, maximum, or average value. Gaps smaller than one meter are then filled using a linear interpolation. Bare earth and first return rasters were created using this procedure with the averaging option selected for cells with multiple values. Both of these maps were exported in the ESRI® grid format for import into ArcGIS®. Both rasters were gridded at 1-meter per pixel resolution.

Classification of multispectral imagery

Two types of multispectral imagery were used to assess the range and density of redcedar. Initially, a coarse (30-meter spatial resolution) Landsat classification was used to identify areas of redcedar cover. This classification ensured that areas of significant closed-canopy redcedar cover would be identified. It also provided a means of delineating the areas to be classified within the higher resolution data. The second round of multispectral classification involved the hybrid use of U.S. Department of Agriculture National Agricultural Imagery Program (NAIP) 4-band (NIR-R-G-B) data and LiDAR. Within areas already identified as containing redcedar based on the coarser Landsat classification, a second classification was derived from the higher resolution NAIP data. This allowed for a more accurate estimate of redcedar density and resulted in a 1-meter spatial resolution classification of redcedar that was subsequently used to identify the target species in a 1-meter LiDAR-derived canopy height model.

Unsupervised classification of Landsat imagery

A multi-temporal classification technique was performed using cloud-free Landsat TM images from January 5, 2011 and August 1, 2011, which represented winter and summer dates, respectively. Six bands from each image (omitting the thermal band) were stacked using ERDAS Imagine© software. The resulting 12-band image (see Figure 2.3) was used as the input in the ISODATA unsupervised classifier tool in ERDAS Imagine. We specified that the output be 50 clusters with a confidence interval of 0.95. The resulting 50 spectral clusters were manually interpreted by comparing them with ground truth data and high-resolution NAIP imagery. We used a modified Anderson Level I classification scheme (Anderson, 1976) to classify each cluster. We separated the Level I “forest land” class into “deciduous forest land” and “evergreen forest land” as indicated in level 2 of the Anderson scheme. This separation was preferred since evergreen forest in the study area is almost exclusively comprised of eastern redcedar, the target land cover type. The clusters that were interpreted to include redcedar cover were identified and extracted. In an iterative process known as “cluster busting,” ISODATA was used again to further refine the redcedar classification (Jensen, 2005).

During cluster busting, the analyst identifies the clusters that include or that are most spectrally similar to the target land cover type. All other clusters are masked out, and ISODATA is performed a second time. This process often finds “hidden” spectral information that can reveal other land cover types in the image that were not evident in the initial ISODATA classification. Multiple iterations of cluster busting are sometimes necessary to accurately extract a particular land cover type, as was the case in extracting redcedar cover. For this study, two iterations were necessary to separate redcedar from other cover types. After redcedar was accurately classified, the classification accuracy was assessed using a simple random sampling scheme to visually compare the classified Landsat pixels with high resolution NAIP imagery in which redcedar cover was more obvious.

Classification of higher spatial resolution NAIP imagery

USDA NAIP four-band data from 2008 were obtained from DASC. NAIP data were not available with a near-infrared band in the raw format for the same time period as the LIDAR collection and therefore a decision was made to use the closest possible collection. The spatial resolution of the data was 1-meter and the data had been orthorectified. Multispectral data were

co-registered to the LiDAR canopy models to ensure proper alignment (RMS error smaller than one pixel). Prior to classification of NAIP data, all areas within the imagery corresponding with areas in the canopy height model below 0.5 meters were masked out. This removed any remaining water pixels and shadow on the ground, both of which were easily confused with dark shadowed redcedar spectral values in the data. An unsupervised classification was then conducted for all areas classified as redcedar in the initial Landsat classification.

Once again, the ISODATA classification algorithm was used to produce 50 clusters. Clusters were visually interpreted and assigned to redcedar and non-redcedar classes. User's accuracy was calculated using 100 randomly selected validation samples, which were evaluated using a combination of site survey and imagery interpretation. Percent cover by redcedar was calculated from the classified NAIP data for each of the 17 study sites using the ArcGIS® zonal statistics tool.

Redcedar canopy model development

Development of a biomass prediction model for redcedar first necessitated the removal of other aboveground structures and tree species from the canopy height raster. This was accomplished by the creation of a 1-meter resolution redcedar binary mask from the classified image data. The application of this mask resulted in a canopy height model representative of only redcedar canopy height.

The ArcGIS® zonal statistics tool was used to calculate the following summary statistics of the canopy height model for each of the 17 study sites: sum of canopy height, mean canopy height, median canopy height, maximum canopy height, minimum canopy height, and standard deviation of canopy height. Zeros were not included in the calculation of zonal statistics pertaining to the canopy height model. The exclusion of zeros allowed for the calculation of a more accurate measure of mean canopy height.

Biomass predictive model and map development

Development of a predictive statistical model for biomass began with the extraction of metrics for each field site area from both the canopy height model and redcedar classification. These metrics were: percent cover by redcedar derived from classification map, sum of canopy height, mean canopy height, median canopy height, maximum canopy height, minimum canopy height, and standard deviation of canopy height. Stepwise linear ordinary least squares regression

was used to determine the most accurate model for biomass prediction using these parameters. Models were evaluated on Root Mean Squared Error, Bayesian information criterion, and coefficient of determination.

After a predictive equation was developed, a map of redcedar biomass was calculated using ArcGIS® spatial modeler. First, the ArcGIS® block statistics tool was used to calculate percent cover of redcedar within a 15x15-meter window. The same procedure was also used to calculate mean canopy height within a 15x15-meter window. A weighted overlay was then used to calculate a 15-meter resolution biomass raster. The resulting map was resampled to 30-meter and 60-meter resolution in both short (imperial) tons and metric tons for dissemination to interested parties.

Results

Redcedar Canopy Model

Figure 4.5 shows the resulting equation relating diameter at breast height (DBH) to tree biomass. This equation was used to calculate biomass for each ground control site. Statistics include average tree age, maximum tree age, and mean tree height of selected trees as well as percent cover by redcedar (calculated from densiometer readings) and biomass (calculated as a sum of tree biomass for each site derived from diameter at breast height and the allometric equation).

A strong relationship was found between the redcedar canopy height model (derived from a LiDAR-based canopy height model and classification of NAIP imagery) and the mean tree height of selected trees in ground reference plots (Figure 4.7). The strength of this relationship suggests that LiDAR is a reliable measure of canopy height and that the use of NAIP to remove non-target species was not detrimental to this relationship. There was also a strong relationship between the percentage of redcedar cover as calculated from the classified NAIP data and the percentage estimated on the ground using densiometer readings (Figure 4.8).

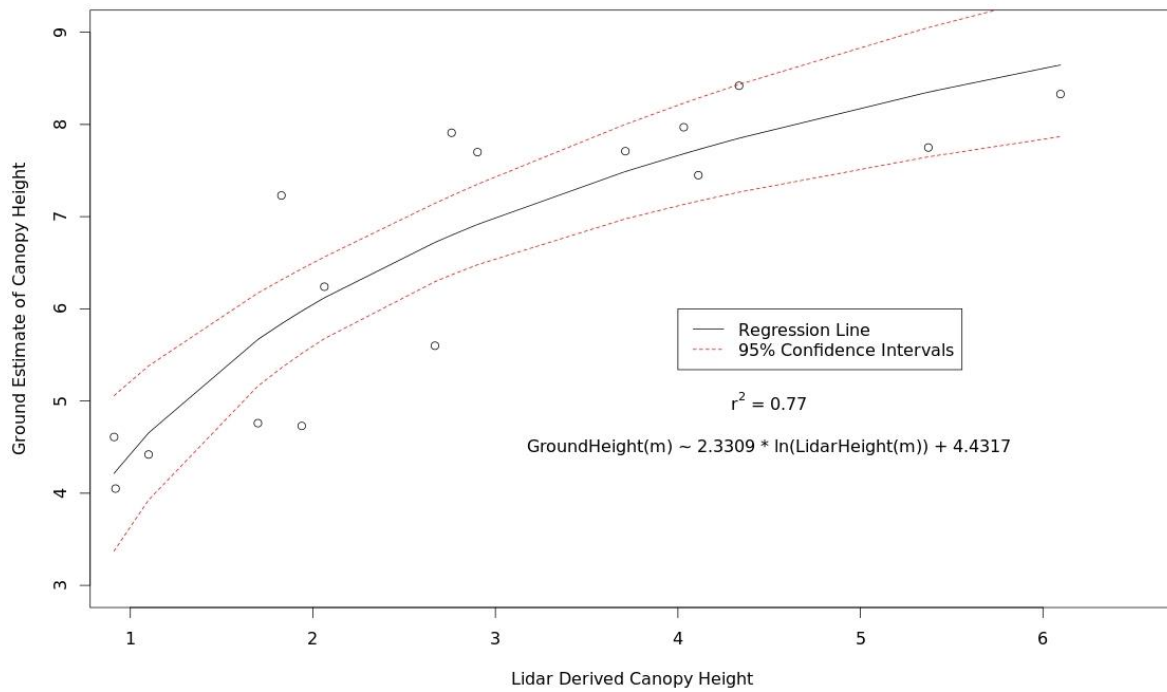


Figure 4.7 Redcedar canopy height model (LiDAR) vs. mean redcedar height in ground reference plots.

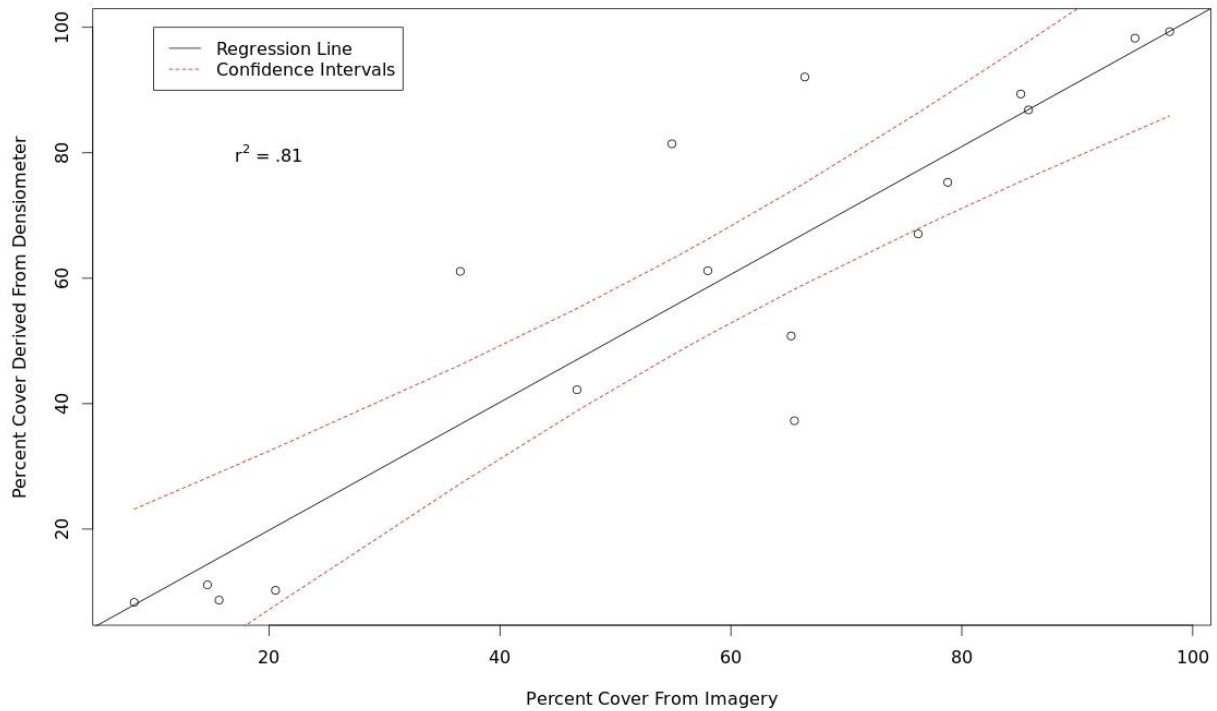


Figure 4.8 Aerial percent cover vs. ground canopy cover (measured with densiometer).

Biomass Predictive Model

Stepwise model selection using a forward and backward model selection with AIC as the selection criterion found that mean canopy height, derived from LiDAR, and percent cover, derived from classified imagery, were the best predictors of redcedar biomass. This model also produced the lowest residual sum of squares and subsequently the lowest root mean square error (RSME).

An accuracy assessment of the final model is shown in Table 4.2. The final model was developed and tested in the Weka® data mining software and k-folds cross validation was used to test model accuracy. The model's root-mean squared error was approximately 35 megagrams (metric tons) per hectare.

Table 4.2 Accuracy assessment summary of the redcedar biomass prediction model.

Equation	R-Squared	Root Mean Squared Error	Root Relative Squared Error
Biomass = 3655.48 * NAIP Derived Percent Cover + 602.02 * LiDAR Derived Mean Canopy Height – 676.03	0.72	35 Megagrams/Hectare or 792 kg/ 225 m ² plot	51 %

Conclusion

The combined use of LiDAR and multispectral remotely sensed data was again shown to be an effective method of assessing the biomass of a target species within a heterogeneous landscape. It is therefore well-suited for monitoring the encroachment of undesirable woody species. Model error, as measured by root mean square error, was within the range of previous models developed to predict biomass using LiDAR data (Drake *et al.*, 2003). A possible source of error includes the incongruence between the dates of collection for remotely sensed and ground reference data. Another potential source of error is the coarse point spacing of the LiDAR. Future work includes expanding the study to other areas prone to redcedar encroachment, improving model accuracy by simultaneous collection of ground reference and remotely sensed data, and exploration of other LiDAR-based forest inventory techniques such as individual tree extraction. Tighter LiDAR point spacing could allow for better characterization of crown shape and allow for individual tree-based approaches to be used.

References

1. Allen, M. S. and M. W. Palmer. 2011. "Fire history of a prairie/forest boundary: more than 250 years of frequent fire in a North American tallgrass prairie." *Journal of Vegetation Science* 22(3): 436–444.
2. Anderson, J. R., E. E. Hardy, J. T. Roach, and R. E. Witmer. 1976. *A Land Use and Land Cover Classification System For Use With Remote Sensor Data*. Washington, D.C.: United States Government Printing Office.
3. Ansley, R. J., M. Mirik, B. W. Surber, and S. C. Park. 2012. "Canopy Area and Aboveground Mass of Individual Redberry Juniper (*Juniperus pinchotii*) Trees." *Rangeland Ecology and Management* 65(2): 189–195.
doi: <http://dx.doi.org/10.2111/REM-D-11-00112.1>
4. Bechtold, W. A. and P. L. Patterson. 2005. "The Enhanced Forest Inventory and Analysis Program—National Sampling Design and Estimation Procedures." *USDA Forest Service Publication SRS-80*.
5. Blatchley, W. S. 1912. *The Indiana weed book*. Nature Publishing Company.
6. Booth, D. T. and P. T. Tueller. 2003. "Rangeland Monitoring Using Remote Sensing." *Arid Land Research and Management* 17: 455–467.
doi: 10.1080/15324980390225539.
7. Bortolot, Z. J., and R. H. Wynne. 2005. "Estimating Forest Biomass Using Small Footprint Lidar Data: an Individual Tree-Based Approach That Incorporates Training Data." *ISPRS Journal of Photogrammetry and Remote Sensing* 59 (6): 342–360.
8. Bragg, T. B. and L. C. Hulbert. 1976. "Woody Plant Invasion of Unburned Kansas Bluestem Prairie." *Journal of Range Management* 29 (1): 19–24.
9. Briggs, J. M., and D.J. Gibson. 1992. "Effect of Burning on Tree Spatial Patterns in a Tallgrass Prairie Landscape." *Bulletin of the Torrey Botanical Club* 119: 300–307.
10. Briggs, J. M., A. K. Knapp, and B. L. Brock. 2002. "Expansion of Woody Plants in Tallgrass Prairie: A Fifteen-Year Study of Fire and Fire-Grazing Interactions." *American Midland Naturalist* 147 (2): 287–294.
URL: <http://www.jstor.org/stable/3083203>.
11. Briggs, J. M., G. A. Hoch, and L. C. Johnson. 2002. "Assessing the Rate, Mechanisms, and Consequences of the Conversion of Tallgrass Prairie to *Juniperus virginiana* Forest." *Ecosystems* 5 (6): 578–586. doi: 10.1007/s10021-002-0187-4.

12. CAFNRnews. 2008. "Abundant Missouri Tree Might Have Antibiotic, Cancer-Fighting Properties." April 29.
URL: <http://cafnrnews.com/2008/04/abundant-missouri-tree-might-have-antibiotic-cancer-fighting-properties/>
13. Chapman, R. N., D. M. Engle, R. E. Masters, and D. M. Leslie Jr. 2004. "Tree Invasion Constrains The Influence Of Herbaceous Structure In Grassland Bird Habitats." *Ecoscience* 11 (1): 56–63.
14. Drake, J. B., R. G. Knox, R. O. Dubayah, D. B. Clark, R. Condit, J. B. Blair, And M. Hofton. 2003. "Above-Ground Biomass Estimation in Closed Canopy Neotropical Forests Using Lidar Remote Sensing: Factors Affecting the Generality of Relationships." *Global Ecology and Biogeography* 12 (2): 147–159.
15. Everitt, J. H., C. Yang, B. J. Racher, C. M. Britton, and M. R. Davis. 2001. "Remote sensing of redberry juniper in the Texas rolling plains." *Journal of Range Management* 54 (3): 254–259. URL: <http://www.jstor.org/stable/4003243>.
16. Gawde, A. J., Cantrell, C. L., and V. D. Zheljaskov. 2009. Dual extraction of essential oil and podophyllotoxin from *Juniperus virginiana*." *Industrial Crops and Products* 30 (2009): 276–280.
17. Gehring, J. L. and T. B. Bragg. 1992. "Changes in Prairie Vegetation under Eastern Red Cedar (*Juniperus virginiana* L.) in an Eastern Nebraska Bluestem Prairie." *American Midland Naturalist* 128 (2): 209–217. URL: <http://www.jstor.org/stable/2426455>.
18. Grabow, B. and K. P. Price. 2010. Unpublished research, Ecology and Agriculture Spatial Analysis Laboratory (EASAL), Kansas State University.
19. Guo, X., K. P. Price, and J. Stiles. 2003. "Grasslands discriminant analysis using Landsat TM single and multitemporal data." *Photogrammetric Engineering and Remote Sensing* 69 (11): 1255–1262.
20. Hardin, P. J. and M. W. Jackson. 2005. An Unmanned Aerial Vehicle for Rangeland Photography. *Rangeland Ecology & Management* 58(4): 439–442.
21. Hardin, P. J., Jackson, M. W., Anderson, V. J. and Johnson, R. 2007. Detecting Squarrose Knapweed (*Centaurea viregata* Lam. Ssp. *squarrosa* Gugl.) Using a Remotely Piloted Vehicle: A Utah Case Study. *GIScience & Remote Sensing*, 44(3): 203–219.
22. Hemmerly, T. E. 1970. "Economic Uses of Eastern Redcedar." *Economic Botany* 24 (1): 39–41. URL: <http://www.jstor.org/stable/4253106>.
23. Horncastle, V. J., E. C. Hellgren, P. M. Mayer, A. C. Ganguli, D. M. Engle, and D. M. Leslie Jr. 2005. "Implications of Invasion by *Juniperus virginiana* on Small Mammals in The Southern Great Plains." *Journal of Mammalogy* 86 (6): 1144–1155.

24. Jensen, J. R. 1983. "Biophysical Remote Sensing." *Annals of the Association of American Geographers* 73 (1): 111–132. URL: <http://www.jstor.org/stable/2569349>.
25. Jensen, J. R. 2005. *Introductory Digital Image Processing: A Remote Sensing Perspective*. Upper Saddle River: Pearson Prentice Hall.
26. Jensen, J. R. 2007. *Remote Sensing of the Environment: An Earth Resource Perspective*. Upper Saddle River: Pearson Prentice Hall.
27. Kindscher, K. and N. Scott. 1997. "Land Ownership and Tenure of the Largest Land Parcels in the Flint Hills of Kansas, USA." *Natural Areas Journal* 17(2): 131–135.
28. Laliberte, A. S., Herrick, J. E., Rango, A., and C. Winters. 2010. Acquisition, Orthorectification, and Object-based Classification of Unmanned Aerial Vehicle (UAV) Imagery for Rangeland Monitoring. *Photogrammetric Engineering & Remote Sensing*, 76(6): 661-672.
29. Lam, E. 2012. "Effect of Redcedar Oil During Biological Conversion of Eastern Redcedar to Ethanol." Paper presented at the IEEE Green Technologies Conference, Tulsa, April 19–20, 2012.
URL: <http://ieeexplore.ieee.org/stamp/stamp.jsp?tp=&arnumber=6200935>.
30. Langley, S. K., H. M. Cheshire, and K. S. Humes. 2001. "A Comparison of Single Date and Multitemporal Satellite Image Classifications in a Semi-Arid Grassland." *Journal of Arid Environments* 49 (2): 401–411.
doi: <http://dx.doi.org/10.1006/jare.2000.0771>.
31. Little Jr., E. L. 1971. *Conifers and Important Hardwoods*. Vol. 1 of *Atlas of United States Trees*. Washington D.C.: United States Government Printing Office.
32. McCleary, A. L., K. A. Crews-Meyer, and K. R. Young. 2008. "Refining classifications in the western Amazon using an intra-annual multitemporal approach." *International Journal of Remote Sensing* 29 (4): 991–1006.
33. Melgani, F. and L. Bruzzone. 2004. "Classification of Hyperspectral Remote Sensing Images with Support Vector Machines." *IEEE Transactions on Geoscience and Remote Sensing* 42 (8): 1778–1790. doi: 10.1109/TGRS.2004.831865.
34. Mitchell, K. 2010. Quantitative Analysis by the Point-Centered Quarter Method. arXiv preprint arXiv:1010.3303.
35. Moser, W. K., M. H. Hansen, R. L. Atchison, G. J. Brand, B. J. Butler, S. J. Crocker, D. M. Meneguzzo, et al. 2008. *Kansas Forests 2005*. Newtown Square: USDA Forest Service Northern Research Station.

36. Mountrakis, G., J. Im, and C. Ogole. 2011. "Support vector machines in remote sensing: A review." *ISPRS Journal of Photogrammetry and Remote Sensing* 66 (3): 247–259. doi: <http://dx.doi.org/10.1016/j.isprsjprs.2010.11.001>.
37. Norris, M. D., J. M. Blair, and L. C. Johnson. 2001. "Land cover change in eastern Kansas: litter dynamics of closed-canopy eastern redcedar forests in tallgrass prairie." *Canadian Journal of Botany* 79: 214–222.
38. Owensby, C. E., K. R. Blan, B. J. Eaton, and O. G. Russ. 1973. "Evaluation of Eastern Redcedar Infestations in the Northern Kansas Flint Hills." *Journal of Range Management* 26 (4): 256–260. URL: <http://www.jstor.org/stable/3896570>.
39. Owensby, C. E. "Site Characteristics." <http://spuds.agron.ksu.edu/Site.htm>. Accessed on July 17, 2014.
40. Pal, M. and P. M. Mather. 2005. "Support vector machines for classification in remote sensing." *International Journal of Remote Sensing* 26 (5): 1007–1011. doi: 10.1080/01431160512331314083.
41. Pease, J. 2007. "The Perfect Pine?" *Kansas Canopy* 22: 1–3.
42. Peel, M. C., Finlayson, B. L., and T. A. McMahon. 2007. "Updated Köppen-Geiger climate classification map." *Hydrology and Earth System Sciences* 4: 439–473. URL: <http://www.hydrol-earth-syst-sci-discuss.net/4/439/2007/hessd-4-439-2007.pdf>.
43. Popescu, S. C., and R. Wynne. 2004a. "Seeing the Trees in The Forest: Using Lidar and Multispectral Data Fusion With Local Filtering and Variable Window Size for Estimating Tree Height." *Photogrammetric Engineering and Remote Sensing* 70 (5):589-604.
44. Popescu, S. C., R. H. Wynne, and J. A. Scrivani. 2004b. "Fusion of Small-Footprint Lidar and Multispectral Data to Estimate Plot-Level Volume and Biomass in Deciduous and Pine Forests in Virginia, USA." *Forest Science* 50 (4): 551–565.
45. Price, K. P., S. L. Egbert, M. D. Nellis, R. Lee, and R. Boyce. 1997. "Mapping Land Cover in a High Plains Agro-Ecosystem Using a Multidate Landsat Thematic Mapper Modeling Approach." *Transactions of the Kansas Academy of Science* 100 (0.5): 21–33. URL: <http://www.jstor.org/stable/3628436>.
46. Raile, G. K., and J. S. Spencer, Jr. 1984. *Kansas Forest Statistics, 1981*. St. Paul: USDA Forest Service North Central Forest Experiment Station.
47. Raines, J. C., J. Grogan, I. Hung, and J. Kroll. 2008. "Multitemporal analysis using Landsat Thematic Mapper (TM) bands for forest cover classification in east Texas." *Southern Journal of Applied Forestry* 32 (1): 21–27.

48. Ramachandriya, K. D., M. R. Wilkins, S. Hiziroglu, N. T. Dunford, and H. K. Atiyeh. 2013. "Development of an efficient pretreatment process for enzymatic saccharification of Eastern redcedar." *Bioresource Technology* 136: 131–139. doi: <http://dx.doi.org/10.1016/j.biortech.2013.02.056>.
49. Richards, J. A. and X. Jia. 2006. *Remote Sensing Digital Image Analysis*. Berlin: Springer-Verlag.
50. Sankey, T. T. and M. J. Germino. 2008. "Assessment of Juniper Encroachment with the Use of Satellite Imagery and Geospatial Data." *Rangeland Ecology and Management* 61 (4): 412–418. URL: <http://www.jstor.org/stable/25146802>.
51. Sankey, T. T., N. Glenn, S. Ehinger, A. Boehm, and S. Hardegree. 2010. "Characterizing Western Juniper Expansion via a Fusion of Landsat 5 Thematic Mapper and Lidar Data." *Rangeland Ecology and Management* 63 (5): 514–523.
52. Schmidt, T. L. and T. D. Wardle. 2002. "Impact of Pruning Eastern Redcedar (*Juniperus virginiana*)." *Western Journal of Applied Forestry* 17(4): 189–193.
53. Semen, E. and S. Hiziroglu. 2005. "Production, Yield, and Derivatives of Volatile Oils from Eastern Redcedar (*Juniperus Virginiana* L.)." *American Journal of Environmental Sciences* 1 (2): 133–138.
54. Slusher, J. P. 1995. "Wood fuel for heating." In *University of Missouri Extension*. URL: <http://extension.missouri.edu/publications/DisplayPub.aspx?P=G5450>. Accessed on July 21, 2014.
55. Starks, P. J., B. C. Venuto, J. A. Eckroat, and T. Lucas. 2011. "Measuring Eastern Redcedar (*Juniperus virginiana* L.) Mass with the Use of Satellite Imagery." *Rangeland Ecology and Management* 64 (2): 178–186. doi: <http://dx.doi.org/10.2111/REM-D-10-00057.1>
56. Stevens, M, Kaiser, J. and I. Dozier. 2005. "Eastern Red Cedar." *USDA NRCS Plant Guide*. URL: http://plants.usda.gov/plantguide/pdf/cs_juvi.pdf. Accessed on July 21, 2014.
57. Strauss, T., J. Kerschen, C. Morris, K. Friedrichs, M. Zacharias, and S. Watts. 2011. "Relationships between Biophysical and Photogrammetric Measurements of Eastern Redcedar in Northeast Kansas." Student Report at Kansas State University. URL: <http://ces.ksu.org/nres/capstone/RedCedarSpring2011.pdf>.
58. Strine, J. H. 2004. *Windbreaks for Kansas*. Manhattan: Kansas State University.
59. Swatantran, A., R. Dubayah, D. Roberts, M. Hofton, and J. B. Blair. 2011. "Mapping Biomass and Stress in the Sierra Nevada Using Lidar and Hyperspectral Data Fusion." *Remote Sensing of Environment* 115 (11): 2917–2930.

60. Teel, W. S. 2012. "Capturing Heat from a Batch Biochar Production System for Use in Greenhouses and Hoop Houses." *Journal of Agricultural Science and Technology* (2012) 1332–1343.
61. Thayn, J. B., and Price, K. P. 2006. "Estimating Red Cedar Invasion Rates using Landsat and Spectral Matched Filtering." Association of American Geographers Annual Meeting, March 7-11, Chicago, Illinois. (Oral presentation).
62. United States Census Bureau. 2013. "Counties." Geographic data from TIGER. URL: http://tigerweb.geo.census.gov/arcgis/rest/services/TIGERweb/tigerWMS_ACS2013/MapServer/84.
63. United States Department of Agriculture. 2011. "2011 State Agricultural Overview: Kansas." *USDA Publication*.
64. Van Haverbeke, D. F. and R. A. Read. 1976. "Genetics of Eastern Redcedar." *USDA Forest Service Research Paper, US Department of Agriculture*. (WO-32).
65. Ward, E. 2013. "Fire Suppression in Cedar Woodlands." *Kansas State University Research and Extension Publication*.
66. Wing, M. G., Burnett, J., Sessions, J., Brungardt, J., Cordell, V., Dobler, D., and D. Wilson. 2013. "Eyes in the Sky: Remote Sensing Technology Development Using Small Unmanned Aircraft Systems." *Journal of Forestry* 111(5): 341–347.
doi: <http://dx.doi.org/10.5849/jof.12-117>.
67. Wolter, P. T., D. J. Mladenoff, G. E. Host, and T. R. Crow. 1995. "Improved forest classification in the Northern Lake States using multi-temporal Landsat imagery." *Photogrammetric Engineering and Remote Sensing* 61 (9): 1129–1144.
68. Wylie, B. K., D. J. Meyer, M. J. Choate, L. Vierling, P. K. Kozak, And R. O. Green. 2000. "Mapping Woody Vegetation and Eastern Red Cedar in The Nebraska Sand Hills Using AVIRIS." Paper Read at AVIRIS Airborne Geoscience Workshop. JPL Publication 00-18. Pasadena, CA Jet Propulsion Laboratory, California Institute of Technology.